

GREEDY-BASED VALUE REPRESENTATION FOR OPTIMAL COORDINATION IN MULTI-AGENT REINFORCEMENT LEARNING

Lipeng Wan*, Zeyang Liu*, Xingyu Chen, Han Wang, Xuguang Lan

Department of Artificial Intelligence

Xi'an Jiaotong University

wanlipeng@stu.xjtu.edu.cn

ABSTRACT

Due to the representation limitation of the joint Q value function, multi-agent reinforcement learning (MARL) methods with linear or monotonic value decomposition suffer from the relative overgeneralization. As a result, they can not ensure the optimal coordination. Existing methods address the relative overgeneralization by achieving complete expressiveness or learning a bias, which is insufficient to solve the problem. In this paper, we propose the optimal consistency, a criterion to evaluate the optimality of coordination. To achieve the optimal consistency, we introduce the True-Global-Max (TGM) principle for linear and monotonic value decomposition, where the TGM principle can be ensured when the optimal stable point is the unique stable point. Therefore, we propose the greedy-based value representation (GVR) to ensure the optimal stable point via inferior target shaping and eliminate the non-optimal stable points via superior experience replay. Theoretical proofs and empirical results demonstrate that our method can ensure the optimal consistency under sufficient exploration. In experiments on various benchmarks, GVR significantly outperforms state-of-the-art baselines.

1 INTRODUCTION

By taking advantage of the deep learning technique, cooperative multi-agent reinforcement learning (MARL) shows great scalability and excellent performance on challenging tasks (Vorotnikov et al., 2018; Wu et al., 2020) such as StarCraft unit micromanagement (Foerster et al., 2018). As an efficient paradigm of cooperative MARL, centralized training with decentralized execution (CTDE) (Oliehoek et al., 2008; Foerster et al., 2016; Lowe et al., 2017) gains growing attention. A simple and effective approach to adopt CTDE in value-based cooperative MARL is linear value decomposition (LVD) or monotonic value decomposition (MVD). However, both LVD and MVD suffer from relative overgeneralization (Panait et al., 2006; Wei et al., 2018) due to the representation limitation of the joint Q value function. As a result, they can not guarantee optimal coordination.

Recent works address the problem from two different perspectives. The first kind of method aims to solve the representation limitation directly through value functions with complete expressiveness capacity (e.g., QTRAN (Son et al., 2019) and QPLEX (Wang et al., 2020)). However, learning the complete expressiveness is impractical in complicated MARL tasks because the joint action space increases exponentially with the number of agents. The other kind of method tries to overcome relative overgeneralization by learning a bias (e.g., WQMIX (Rashid et al., 2020) and MAVEN (Mahajan et al., 2019)), which lacks theoretical and quantitative analysis of the problem and is only applicable in specific tasks. As a result, these methods

are insufficient to guarantee optimal coordination. More discussions about related works are provided in Appendix B.

Value decomposition is a popular approach to assign credit for individual agents in fully cooperative MARL tasks, where the main concern is the optimality of coordination. In a **successful case** of credit assignment via value decomposition, individual agents act according to their local policies and achieve the best team’s performance. To evaluate value decomposition methods, we propose the **optimal consistency**, a criterion concerning the optimality of coordination. The optimal consistency can be decomposed into two principles: Individual-Global-Max (IGM) and **True-Global-Max (TGM)**.

In this paper, to achieve the optimal consistency efficiently, we investigate the conditions of the TGM principle and go deep into the mechanism of the value representation for LVD and MVD, where the IGM principle always holds. We first derive the expression of the joint Q value function of LVD and MVD, by which we draw some interesting conclusions. **Firstly**, LVD and MVD share the same expression of the joint Q value function. **Secondly**, the joint Q value of any joint action depends on the true Q values of the **whole joint action space**. **Thirdly**, there may be multiple stable points. Each stable point is a possible convergence. However, the TGM principle may be violated in some of the stable points (we call them non-optimal stable points), which are the causes of non-optimal coordination and relative overgeneralization. To ensure the TGM principle in LVD and MVD, the stable point satisfying the TGM principle (we call it the optimal stable point) is required to be the **unique** stable point, which is the target problem to be solved in this paper.

To solve the target problem, we propose the greedy-based value representation (GVR). The optimal point may be unstable for LVD and MVD because its joint Q value depends on the true Q values of the whole action space, for which we propose the inferior target shaping (ITS). ITS removes the dependence by dynamically modifying the true Q value of inferior actions (i.e., the actions with low true Q values) according to current greedy Q value. Besides, under ITS, the non-optimal stable points can be eliminated with a large enough ratio of the probability of superior actions (i.e., the actions better than the greedy) to the greedy action. We prove two simple ways applied by previous works (i.e., improving exploration (Mahajan et al., 2019) and reassigning sample weights (Rashid et al., 2020)) are both inapplicable to raise the ratio because the probabilities of superior actions decreases exponentially with the number of agents. Therefore, we further propose the superior experience replay (SER), where the probabilities of superior actions are independent to environmental parameters. Our method is theoretically proved to ensure the optimal consistency under sufficient exploration.

We have three contributions in this work. (1) This is the first work to derive the general expression of the joint Q value function for LVD and MVD. (2) We propose a quantified condition to ensure optimal consistency in LVD and MVD. (3) We propose the GVR method, which is proved theoretically to ensure the optimal consistency under sufficient exploration, and our method outperforms state-of-the-art baselines in various benchmarks.

2 PRELIMINARIES

2.1 DEC-POMDP

We model a fully cooperative multi-agent task as a decentralized partially observable Markov decision process (Dec-POMDP) described by a tuple $\mathcal{G} = \langle S, U, P, r, Z, O, n, \gamma \rangle$ (Guestrin et al., 2001; Oliehoek & Amato, 2016). $s \in S$ denotes the true state of the environment. At each time step, each agent $a \in A \equiv \{1, 2, \dots, n\}$ receives a local observation $z^a \in Z$ produced by the observation function $O : S \times A \rightarrow Z$, and then chooses an individual action $u^a \in U$ according to a local policy $\pi^a(u^a | \tau^a) : T \times U \rightarrow [0, 1]$, where $\tau^a \in T \equiv (Z \times U)^*$ denotes the local action-observation history. The joint action of n agents \mathbf{u} results in a shared reward $r(s, \mathbf{u})$ and a transition to the next state $s' \sim P(\cdot | s, \mathbf{u})$. $\gamma \in [0, 1]$ is a discount factor.

We denote the joint variable of group agents with bold symbols, e.g., the joint action $\mathbf{u} \in \mathbf{U} \equiv U^n$, the joint action-observation history $\boldsymbol{\tau} \in \mathcal{T} \equiv T^n$, and the **joint interactive policy** (i.e., the policy interacts with environment to generate trajectories) $\pi(\mathbf{u}|\boldsymbol{\tau})$. The **true Q value** is denoted by $\mathcal{Q}(s_t, \mathbf{u}_t) = \mathbb{E}_{s_{t+1:\infty}, \mathbf{u}_{t+1:\infty}} [R_t | s_t, \mathbf{u}_t]$, where $R_t = \sum_{i=0}^{\infty} \gamma^i r_{t+1}$ is the discounted return. The action-state value function of agent a and the group of agents are defined as **utility function** $\mathcal{U}^a(u^a, \tau^a)$ and **joint Q value function** $Q(\mathbf{u}, \boldsymbol{\tau})$ respectively. The true Q value is the target of the joint Q value in training, serving as the unique external criterion of the team’s performance. The **greedy action** $\hat{\mathbf{u}} := \operatorname{argmax}_{\mathbf{u}} Q(\mathbf{u}, \boldsymbol{\tau})$ is defined as the joint action with the maximal joint Q value. The **optimal action** $\mathbf{u}^* := \operatorname{argmax}_{\mathbf{u}} \mathcal{Q}(s, \mathbf{u})$ is defined as the joint action with the best team’s performance. For brevity, we sometimes omit the prefix ”joint” for the joint variables.

2.2 OPTIMAL CONSISTENCY AND TGM PRINCIPLE

In CTDE paradigm, agents are expected to act individually according to their local policies (i.e., the individual greedy actions) while achieve the optimal coordination (i.e., the maximal true Q value). Here we define the correspondence between the individual greedy actions and the maximal true Q value as the optimal consistency.

Definition 1 (Optimal consistency). Given a set of utility functions $\{\mathcal{U}^1(u^1, \tau^1), \dots, \mathcal{U}^n(u^n, \tau^n)\}$, and the true Q value $\mathcal{Q}(s, \mathbf{u})$, if the following holds

$$\{\operatorname{argmax}_{u^1} \mathcal{U}^1(u^1, \tau^1), \dots, \operatorname{argmax}_{u^n} \mathcal{U}^n(u^n, \tau^n)\} = \operatorname{argmax}_{\mathbf{u}} \mathcal{Q}(s, \mathbf{u}) \quad (1)$$

then we say the set of utility functions $\{\mathcal{U}^1(u^1, \tau^1), \dots, \mathcal{U}^n(u^n, \tau^n)\}$ satisfies the optimal consistency. For simplicity, we ignore situations with non-unique optimal actions.

The optimal consistency can be decomposed into two principles: Individual-Global-Max (IGM) and True-Global-Max (TGM). The IGM principle proposed by QTRAN (Son et al., 2019) is defined on the correspondence between individual greedy actions and the joint greedy actions (formally, $\{\operatorname{argmax}_{u^1} \mathcal{U}^1(u^1, \tau^1), \dots, \operatorname{argmax}_{u^n} \mathcal{U}^n(u^n, \tau^n)\} = \operatorname{argmax}_{\mathbf{u}} Q(\mathbf{u}, \boldsymbol{\tau})$). To achieve the optimal consistency, the correspondence between the joint greedy action and the maximal true Q value is required, for which we define the TGM principle:

Definition 2 (TGM). Given a joint value function $Q(\mathbf{u}, \boldsymbol{\tau})$, and the true Q value $\mathcal{Q}(s, \mathbf{u})$, if the following holds

$$\operatorname{argmax}_{\mathbf{u}} Q(\mathbf{u}, \boldsymbol{\tau}) = \operatorname{argmax}_{\mathbf{u}} \mathcal{Q}(s, \mathbf{u}) \quad (2)$$

then we say the joint value function $Q(\mathbf{u}, \boldsymbol{\tau})$ satisfies the TGM principle. For simplicity, we ignore situations with non-unique optimal actions.

3 INVESTIGATION OF THE TGM PRINCIPLE FOR LVD & MVD

Linear value decomposition (LVD) and monotonic value decomposition (MVD) are simple and naturally meet the IGM principle (Son et al., 2019). To achieve the optimal consistency, we investigate the conditions of the TGM principle for LVD and MVD. According to Def.2, the TGM principle is related to the joint Q value function $Q(\mathbf{u}, \boldsymbol{\tau})$. In this section, we first derive the expression of $Q(\mathbf{u}, \boldsymbol{\tau})$ for LVD and MVD under ϵ -greedy visitation. The expression indicates there may be non-optimal stable points which violate the TGM principle. To ensure the TGM principle, the optimal stable point must be the unique stable point, for which we propose a quantified sufficient condition.

3.1 EXPRESSION OF THE JOINT Q VALUE FUNCTION FOR LVD & MVD

Firstly, take two-agent linear value decomposition as an example, where the joint Q value function $Q(u_i^1, u_j^2, \tau)$ is linearly factorized into two utility functions $Q(u_i^1, u_j^2, \tau) = \mathcal{U}^1(u_i^1, \tau^1) + \mathcal{U}^2(u_j^2, \tau^2)$. $u_i^1, u_j^2 \in \{u_1, \dots, u_m\}$ denote the individual actions of agent 1,2 respectively, where $\{u_1, \dots, u_m\}$ is the discrete individual action space. Specially, we denote the individual greedy action of agent 1,2 with \hat{u}^1, \hat{u}^2 respectively. Through the derivation provided in Appendix C.1, Q_{ij} can be represented by the true Q values as

$$Q(u_i^1, u_j^2, \tau) = \frac{\epsilon}{m} \sum_{k=1}^m [\mathcal{Q}(s, u_i^1, u_k^2) + \mathcal{Q}(s, u_k^1, u_j^2)] + (1 - \epsilon) [\mathcal{Q}(s, \hat{u}^1, u_j^2) + \mathcal{Q}(s, u_i^1, \hat{u}^2)] - \frac{\epsilon^2}{m^2} \sum_{i=1}^m \sum_{j=1}^m \mathcal{Q}(s, u_i^1, u_j^2) - \frac{\epsilon(1 - \epsilon)}{m} \sum_{k=1}^m [\mathcal{Q}(s, \hat{u}^1, u_k^2) + \mathcal{Q}(s, u_k^1, \hat{u}^2)] - (1 - \epsilon)^2 \mathcal{Q}(s, \hat{u}^1, \hat{u}^2) \quad (3)$$

Verification of the expression is provided in Appendix C.2. For monotonic value decomposition, the expression is identical to Eq.3 (the proof is provided in Appendix D), which indicates the coefficients and bias on utility functions do not affect the joint Q value function. For situations with more than two agents, by referring to the derivation in Appendix C.1 and D, the expression of joint Q values can also be obtained.

3.2 A SUFFICIENT CONDITION TO ENSURE THE TGM PRINCIPLE FOR LVD & MVD

According to Eq.3, **the joint Q values** $Q(u, \tau) (u = \{u_i^1, u_j^2\})$ **depends on the greedy action** $\hat{u} = \{\hat{u}^1, \hat{u}^2\}$. An example of the relationship between $Q(u, \tau)$ and \hat{u} is shown in Fig.1, where $\epsilon = 0.2$.

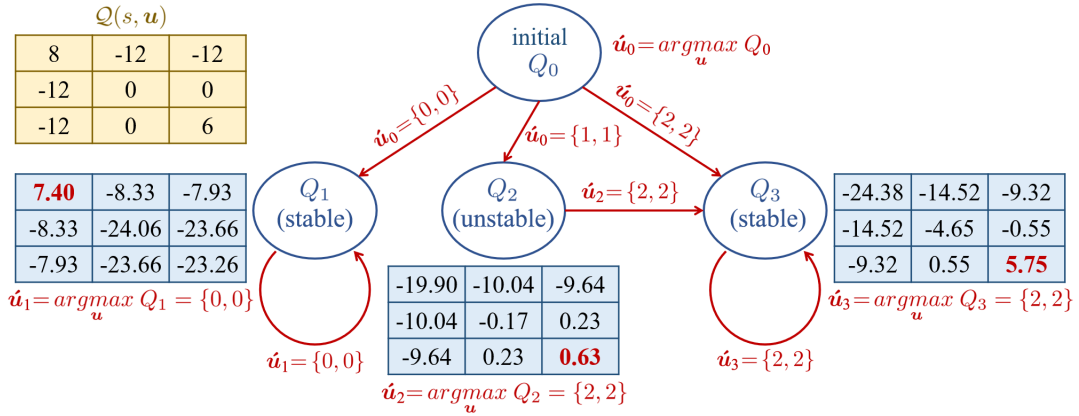


Figure 1: Relationship between $Q(u, \tau)$ (blue tables, calculated by Eq.3) and the greedy action \hat{u} . The true Q values $\mathcal{Q}(s, u)$ is shown in the yellow table. Initial $Q(u, \tau) = Q_0$ transfers to different points (i.e., Q_1, Q_2, Q_3) according to the corresponding greedy action $\hat{u}_0 = \arg\max_u Q_0$. We omit the other cases of \hat{u}_0 such as $\hat{u}_0 = \{0, 1\}$ and $\hat{u}_0 = \{2, 0\}$.

In Fig.1, $Q(u, \tau)$ is trained to approximate the $\mathcal{Q}(s, u)$, where the loss function is defined as the expectation on representation error, i.e., $loss = \mathbb{E}_{u \sim \pi(u|\tau)} [Q(u, \tau) - \mathcal{Q}(s, u)]$. Due to the representation limitation of $Q(u, \tau)$ for LVD and MVD, $\forall u \in \mathcal{U}, Q(u, \tau) \neq \mathcal{Q}(s, u)$. Notice that Q_2 is unstable, since it finally transfers to Q_3 . Here we define the stable point of LVD and MVD.

Definition 3 (Stable point of LVD and MVD). Given a linear (or monotonic) factorized joint Q value function $Q(\mathbf{u}, \tau)$ with the minimum loss $loss = \mathbb{E}_{\mathbf{u} \sim \pi(\mathbf{u}|\tau)} [Q(\mathbf{u}, \tau) - \mathcal{Q}(s, \mathbf{u})]$, where $\mathcal{Q}(s, \mathbf{u})$ is the true Q values and $\pi(\mathbf{u}|\tau)$ is the interactive policy, if the following holds

$$\underset{\mathbf{u}}{\operatorname{argmax}} Q(\mathbf{u}, \tau) = \underset{\mathbf{u}}{\operatorname{argmax}} \pi(\mathbf{u}|\tau) \quad (4)$$

then we say $Q(\mathbf{u}, \tau)$ and the greedy action $\hat{\mathbf{u}} = \underset{\mathbf{u}}{\operatorname{argmax}} Q(\mathbf{u}, \tau)$ are stable, and $\{Q(\mathbf{u}, \tau), \hat{\mathbf{u}}\}$ is a **stable point** of LVD (or MVD). Specially, if $\{Q(\mathbf{u}, \tau), \hat{\mathbf{u}}\}$ is a stable point and $\hat{\mathbf{u}} = \mathbf{u}^*$, we say $\{Q(\mathbf{u}, \tau), \hat{\mathbf{u}}\}$ is the **optimal stable point**, otherwise (i.e., $\{Q(\mathbf{u}, \tau), \hat{\mathbf{u}}\}$ is a stable point but $\hat{\mathbf{u}} \neq \mathbf{u}^*$) we say $\{Q(\mathbf{u}, \tau), \hat{\mathbf{u}}\}$ is a **non-optimal stable point**, where \mathbf{u}^* is the optimal action.

Notice that $\pi(\mathbf{u}|\tau)$ is the action distribution of samples for training, and $Q(\mathbf{u}, \tau)$ is the training result on such samples. For example, consider the case $\hat{\mathbf{u}}_0 = \{1, 1\}$ in Fig.1, $\underset{\mathbf{u}}{\operatorname{argmax}} \pi(\mathbf{u}|\tau) = \hat{\mathbf{u}}_0 = \{1, 1\}$ while $\underset{\mathbf{u}}{\operatorname{argmax}} Q_2 = \hat{\mathbf{u}}_2 = \{2, 2\}$. According to Def.3, Q_2 is unstable because $\underset{\mathbf{u}}{\operatorname{argmax}} \pi(\mathbf{u}|\tau) \neq \underset{\mathbf{u}}{\operatorname{argmax}} Q_2$. Q_1 and Q_3 are both stable. Specially, $\{Q_3, \hat{\mathbf{u}}_3\}$ is a non-optimal stable point since $\hat{\mathbf{u}}_3 = \{2, 2\} \neq \mathbf{u}^* = \{0, 0\}$. More discussion about the stable points is provided in Appendix J.

Each stable point is a possible convergence. However, according to Def.2 and Def.3, **the non-optimal stable points violate the TGM principle** because $\hat{\mathbf{u}} = \underset{\mathbf{u}}{\operatorname{argmax}} Q(\mathbf{u}, \tau) \neq \mathbf{u}^* = \underset{\mathbf{u}}{\operatorname{argmax}} \mathcal{Q}(s, \mathbf{u})$. To ensure the TGM principle, **the optimal stable point must be the unique stable point**, i.e., the optimal point is stable and all non-optimal points are unstable. A sufficient condition to ensure the optimal stable point is $\forall \mathbf{u}_s \neq \hat{\mathbf{u}}$, if $\mathcal{Q}(s, \mathbf{u}_s) \leq \mathcal{Q}(s, \hat{\mathbf{u}})$, $Q(\mathbf{u}_s, \tau) < Q(\hat{\mathbf{u}}, \tau)$ holds. Similarly, a sufficient condition to eliminate all non-optimal stable points is $\forall \mathbf{u}_s \neq \hat{\mathbf{u}}$, if $\mathcal{Q}(s, \mathbf{u}_s) > \mathcal{Q}(s, \hat{\mathbf{u}})$, $Q(\mathbf{u}_s, \tau) > Q(\hat{\mathbf{u}}, \tau)$ holds. As a result, a sufficient condition to ensure the TGM principle is given in Remark 1.

Remark 1 (A sufficient condition to ensure the TGM principle). Given a greedy action $\hat{\mathbf{u}} = \underset{\mathbf{u}}{\operatorname{argmax}} \pi(\mathbf{u}|\tau)$, for $\forall \mathbf{u}_s \neq \hat{\mathbf{u}}$

$$\begin{cases} \Delta Q(\mathbf{u}_s, \tau) < 0 & \Delta \mathcal{Q}(s, \mathbf{u}_s) \leq 0 \\ \Delta Q(\mathbf{u}_s, \tau) > 0 & \Delta \mathcal{Q}(s, \mathbf{u}_s) > 0 \end{cases} \quad (5)$$

where $\pi(\mathbf{u}|\tau)$ is the interactive policy, $\Delta \mathcal{Q}(s, \mathbf{u}_s) = \mathcal{Q}(s, \mathbf{u}_s) - \mathcal{Q}(s, \hat{\mathbf{u}})$ and $\Delta Q(\mathbf{u}_s, \tau) = Q(\mathbf{u}_s, \tau) - Q(\hat{\mathbf{u}}, \tau)$. Explanations about the condition are provided in Appendix E.

4 METHOD

To ensure the TGM principle for LVD and MVD, the optimal stable point must be the unique stable point, for which we propose the greedy-based value representation (GVR). The optimal point may be unstable for LVD and MVD because its joint Q value depends on the true Q values of the whole action space. To stabilize the optimal point, we first propose inferior target shaping (ITS) which removes the dependence. Besides, we prove that under ITS, the non-optimal stable points can be eliminated with a large enough ratio of the probability of superior actions to the greedy action. However, general methods (e.g., improving exploration and reassigning sample weights) raising the ratio are ineffective since the probability of superior actions decreases exponentially as the number of agents grows. To eliminate the non-optimal stable points, we further propose superior experience replay, where the probability of superior actions is large enough and almost independent from the environmental parameters (e.g., the number of agents).

4.1 INFERIOR TARGET SHAPING

According to Eq.3, the joint Q value of any action depends on the true Q values of the whole joint action space for LVD and MVD. As a result, the stability of a greed action depends on the true Q values of other actions. Firstly, we consider to remove the dependence. Because the exact true Q values of non-optimal

actions are uninformative, we only represent the "non-optimality" of these samples. Here we propose the ITS target $\mathcal{Q}_{its}(s, \mathbf{u})$

$$\mathcal{Q}_{its}(s, \mathbf{u}) = \begin{cases} Q(\hat{\mathbf{u}}, \tau) - \alpha|Q(\hat{\mathbf{u}}, \tau)| & \mathcal{Q}(s, \mathbf{u}) \leq \mathcal{Q}(\hat{\mathbf{u}}, \tau) * (1 + e_{Q0}) \text{ and } \mathbf{u} \neq \hat{\mathbf{u}} \\ \mathcal{Q}(s, \mathbf{u}) & \text{others} \end{cases} \quad (6)$$

The actions in the first case are called **inferior actions**. α is a hyper-parameter and $\alpha > 0$. A large enough α prevents the confusion between the greedy and inferior actions. e_{Q0} is the the true Q value's minimum tolerable error of a non-optimal action and $e_{Q0} \geq 0$. Besides, the action \mathbf{u} which satisfies $\mathcal{Q}(s, \mathbf{u}) > \mathcal{Q}(s, \hat{\mathbf{u}}) * (1 + e_{Q0})$ and $\mathbf{u} \neq \hat{\mathbf{u}}$ is called **superior action**. To distinguish superior and inferior actions, we first introduce a critic $V(s)$ which approximates $\mathcal{Q}(s, \mathbf{u}) * (1 + e_{Q0})$. The target of the critic is

$$\mathcal{V}_{gvr}(s) = \begin{cases} \mathcal{Q}(s, \mathbf{u}) * (1 + e_{Q0}) & \mathbf{u} = \hat{\mathbf{u}} \\ V(s) & \mathbf{u} \neq \hat{\mathbf{u}} \end{cases} \quad (7)$$

Examples of ITS target is provided in Appendix I. ITS simplifies the representation since the exact true Q value of the inferior actions are ignored. Under ITS, given the greedy action $\hat{\mathbf{u}}$ and any other action $\mathbf{u}_s (\mathbf{u}_s \neq \hat{\mathbf{u}})$, assuming $\mathcal{Q}(s, \hat{\mathbf{u}}) > 0$, we have

$$\Delta Q(\mathbf{u}_s, \tau) = Q(\mathbf{u}_s, \tau) - Q(\hat{\mathbf{u}}, \tau) = n(\eta_1 - \eta_2) [\mathcal{Q}(s, \hat{\mathbf{u}}) - (1 - \alpha)Q(\hat{\mathbf{u}}, \tau)] + n\eta_1 e_Q \mathcal{Q}(s, \hat{\mathbf{u}}) \quad (8)$$

where $e_Q = \frac{\mathcal{Q}_{its}(s, \mathbf{u}_s) - \mathcal{Q}(s, \hat{\mathbf{u}})}{\mathcal{Q}(s, \hat{\mathbf{u}})}$, $\eta_1 = (\frac{\epsilon}{m})^{n-1}$, and $\eta_2 = (1 - \epsilon + \frac{\epsilon}{m})^{n-1}$. We provide two different versions of proof for Eq.8 in Appendix F, and the calculation result is verified in the experimental part (Fig.2(a)).

Suppose $\hat{\mathbf{u}}$ is the optimal action, i.e., $\hat{\mathbf{u}} = \mathbf{u}^*$, it can be proved (in Appendix F.1) that $\Delta Q(\mathbf{u}_s, \tau) < 0$ for $\forall \mathbf{u}_s \neq \mathbf{u}^*$. According to Remark 1, **the optimal point is always stable**. Besides, suppose $\hat{\mathbf{u}}$ is a non-optimal action, i.e., $\exists \mathbf{u}_s$ such that $\mathcal{Q}(s, \mathbf{u}_s) > \mathcal{Q}(s, \hat{\mathbf{u}})$. To destabilize it, let $\Delta Q(\mathbf{u}_s, \tau) > 0$, $e_{Q0} = 0$, and assume $\mathcal{Q}(\hat{\mathbf{u}}, \tau) \approx \mathcal{Q}(s, \hat{\mathbf{u}})$ (this assumption is quite accurate, as verified in Appendix G.2), we have

$$\frac{\eta_1}{\eta_2} > \frac{\alpha}{\alpha + e_Q} \quad (9)$$

which indicates the non-optimal stable points can be eliminated by raising $\frac{\eta_1}{\eta_2}$ under ITS. A simple way to achieve this is **improving exploration**. Substituting the expression of η_1 and η_2 into Eq.9, we have

$$\epsilon > \frac{m}{(\frac{e_Q}{\alpha})^{\frac{1}{n-1}} + 1 + m - 1} \quad (10)$$

When $\mathbf{u}_s = \mathbf{u}^*$, we obtain the **lower bound of ϵ** (denoted by ϵ_0) from the right side of Eq.10. However, as the number of agents n and the size of individual action spaces m increases, ϵ_0 grows close to 1 (an example is provided in Fig.2(b)), which is inapplicable in tasks with long episodes.

Another way is **applying a weight $w (w > 1)$ to the loss of superior actions**. It is proved in Appendix G.1 that the non-optimal stable points can be eliminated when $w > w_0$, where $w_0 = \frac{\alpha(\eta_2 - \eta_1)}{e_Q \eta_1}$ is the lower bound of w . However, w_0 grows exponentially as the number of agents n increases (as verified in Appendix G.2, $w_0 = 659.50$ when $n = 4$), which introduces instability in training.

4.2 SUPERIOR EXPERIENCE REPLAY

$\frac{\eta_1}{\eta_2}$ decreases exponentially as the the number of agents n grows. However, the required lower bound of $\frac{\eta_1}{\eta_2}$ is a constant (i.e., $\frac{\alpha}{\alpha + e_Q}$). We consider adding a constant to η_1 , i.e., adding a constant to the probability of the superior actions.

Inspired by prioritized experience replay (Schaul et al., 2015; Zhang & Sutton, 2017), we introduce a superior buffer. The number of samples with superior actions within a trajectory is defined as the priority of the

trajectory. In the superior buffer, trajectories are ranked according to their priorities. The training batch consists of two parts: trajectories randomly sampled from the replay buffer and the top k trajectories from the superior buffer. At the end of each episode, the trajectories in the training batch will be stored into the superior buffer after the update of their priorities. The working principle of GVR and the algorithm is given in Appendix I.

The probabilities of superior actions are very small in replay buffer. As a result, the proportions of superior actions in the training batch are mainly determined by the weight w of samples from the superior buffer, which is a constant. It is proved in Appendix H that under ITS, SER can eliminate the non-optimal stable points by selecting a proper weight w where

$$\frac{\eta_2}{1 + e_Q} - \eta_1 \leq w \leq (1 - \alpha)(\eta_2 - \eta_1) \quad (11)$$

5 EXPERIMENTS

In this section, firstly we verify the attributes of stable points for linear value decomposition (LVD) in matrix games, where we also evaluate the improvements of GVR. Secondly, to evaluate the stability and scalability of our method, we test the performance of GVR in predator-prey tasks with extreme reward shaping. Thirdly, we conduct experiments on challenging tasks of StarCraft multi-agent challenge (SMAC) (Samvelyan et al., 2019). Finally, we design ablation studies to investigate the improvement of GVR. Our method is compared with state-of-the-art baselines including QMIX (Rashid et al., 2018), QPLEX (Wang et al., 2020), and WQMIX (Rashid et al., 2020). All results are evaluated over 5 seeds. Additional experiments are provided in Appendix K.

5.1 ONE-STEP MATRIX GAME

Matrix game is a simple fully cooperative multi-agent task, where the shared reward is defined by a payoff matrix. In one-step matrix games, the true Q values are directly accessible from the payoff matrix, which is convenient for the verification of the optimal consistency.

The verification of stable points for LVD. We conduct experiments on two-agent one-step matrix game to verify the expression of joint Q values (i.e., Eq.3). We also verify the effect of reward function and exploration rate ϵ on the stable points. The experimental results and conclusions are provided in Appendix J.

Evaluation of GVR. Since the stability under ITS is determined by Eq.8, we first verify the expression under a random inferior true Q values (\mathcal{Q}). Two payoff matrices of size 3^4 (i.e., $m=3$ and $n=4$) are generated for VDN and ITS respectively:

$$\mathcal{Q}(vdn) = \begin{cases} 6(1 + e_Q) & \mathbf{u} = \{0, 0, 0, 0\} \\ 6 & \mathbf{u} = \{2, 2, 2, 2\} \\ 6(1 - \alpha) & \text{others} \end{cases} \quad \mathcal{Q}(its) = \begin{cases} 6(1 + e_Q) & \mathbf{u} = \{0, 0, 0, 0\} \\ 6 & \mathbf{u} = \{2, 2, 2, 2\} \\ \text{random}(-20, 6) & \text{others} \end{cases} \quad (12)$$

where $e_Q = 0.3$, $\alpha = 0.1$. We measure $\Delta Q(\mathbf{u}^*, \tau) = Q(0, 0, 0, 0) - Q(2, 2, 2, 2)$ for VDN and ITS trained with corresponding matrices, where the greedy action is fixed to $\hat{\mathbf{u}} = \{2, 2, 2, 2\}$. As shown in Fig.2(a), the tested $\Delta Q(\mathbf{u}^*, \tau)$ **consists with our calculation result** ($\Delta Q(\mathbf{u}^*, \tau) = -1.951$) from Eq.8. Besides, $\Delta Q(\mathbf{u}^*, \tau)$ of ITS with random inferior \mathcal{Q} equals to that of VDN with fixed inferior \mathcal{Q} , which suggests that under ITS target, the stable points are **irrelevant** to the return of inferior samples. As a result, ITS largely frees the stable points from the interference of the reward function.

We also evaluate the ratio of optimal stable points for VDN, ITS and GVR as ϵ grows, where the payoff matrices are generated according to $\mathcal{Q}(its)$ (Eq.12) over 5 seeds. At each value of ϵ , 100 times of independent training and test are executed. According to Fig.2(b), for VDN, the optimal point become unstable (i.e.,

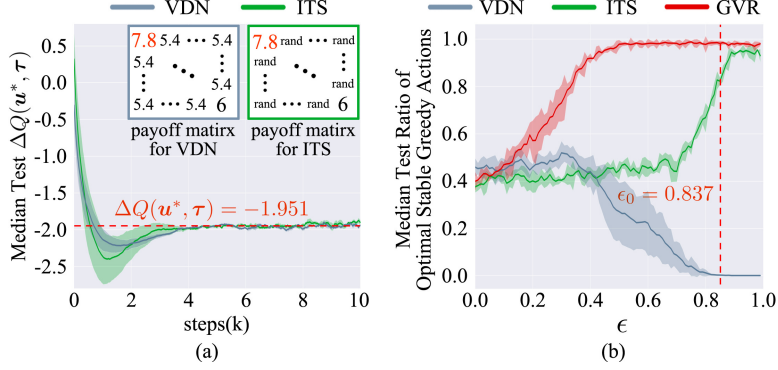


Figure 2: Evaluation of GVR in 4-agent matrix games. (a) Comparison of $\Delta Q(u^*, \tau)$ between ITS with random reward shaping and VDN with fixed reward shaping. The red dash line ($\Delta Q(u^*, \tau) = -1.951$) denotes the calculation result (from Eq.8) under ITS target. (b) Median test ratio of the optimal stable points as ϵ grows (i.e., test probability of the optimal convergence), where $y = 1$ indicates the optimal stable point is the unique stable point and $y = 0$ indicates the optimal point is unstable. The red dash line ($\epsilon_0 = 0.837$) denotes the calculated lower bound of ϵ (from Eq.10) when ITS eliminates non-optimal stable points.

$y = 0$) when $\epsilon > 0.8$. For ITS, the **optimal points is always stable** (i.e., $y > 0 (\forall \epsilon \in (0, 1])$). Besides, ITS eliminates most of the non-optimal stable points under **large exploration** ($\epsilon > 0.837$), which **consists with our calculation result** (the red dash line) from Eq.10. For GVR, the optimal stable point is the unique stable point (i.e., the optimal consistency holds) under a wild range of ϵ . However, GVR is unable to ensure the optimal consistency under a small ϵ , where the optimal sample is not explored in given training steps (e.g., the probability of the optimal sample $u^* = \{0, 0, 0, 0\}$ is $1.98e - 5$ under the greedy action $\hat{u} = \{2, 2, 2, 2\}$).

GVR vs methods with complete expressiveness capacity. To compare the efficiency between GVR and methods with complete expressiveness capacity, we evaluate GVR, QPLEX and CWQMIX in matrix games with different scales of action space. Similar to $Q(its)$ in Eq.12, we generate random matrices of size 3^2 , 6^3 , and 12^4 over 5 seeds, where the first and the last element are set to be 8 and 6 respectively. From Fig.3, in the last two tasks ($U^n = 6^3$ and $U^n = 12^4$), the representation errors of CWQMIX and QPLEX do not decrease during training, which suggests that they are unable to learn the complete expressiveness within given steps. We do not measure the representation error of GVR because the representation target is modified by ITS. GVR is the only method ensuring the optimal coordination (i.e. median test return = 8).

5.2 PREDATOR-PREY

In this subsection, we compare GVR with state-of-the-art baselines in the predator-prey tasks (Böhmer et al., 2020). In our experiments, 8 predators are trained to capture 8 preys, where the preys are controlled by random policies. The reward is shared by all predators, and a punishment is applied to the reward when only a single agent capture a prey. Our experiments are carried out under 3 punishment values.

From Fig.4, VDN and QMIX fail in all experiments, where all agents tend to avoid the preys. QPLEX also fails in spite of its complete expressiveness capacity. WQMIX can only solve the task with a small punishment of -2, while GVR is able to solve the tasks under all punishments.

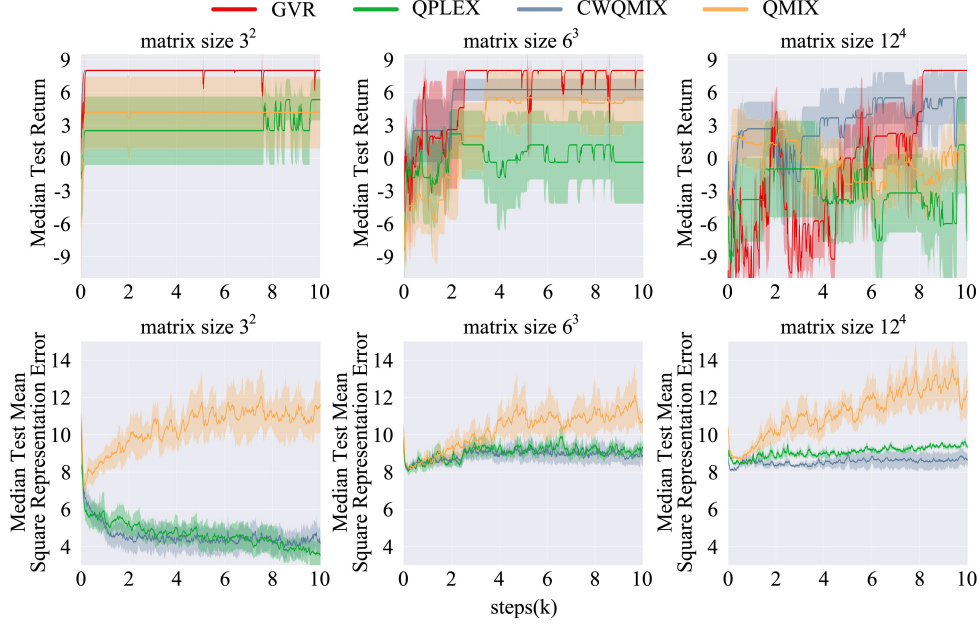


Figure 3: GVR vs methods with complete expressiveness capacity in matrix games.

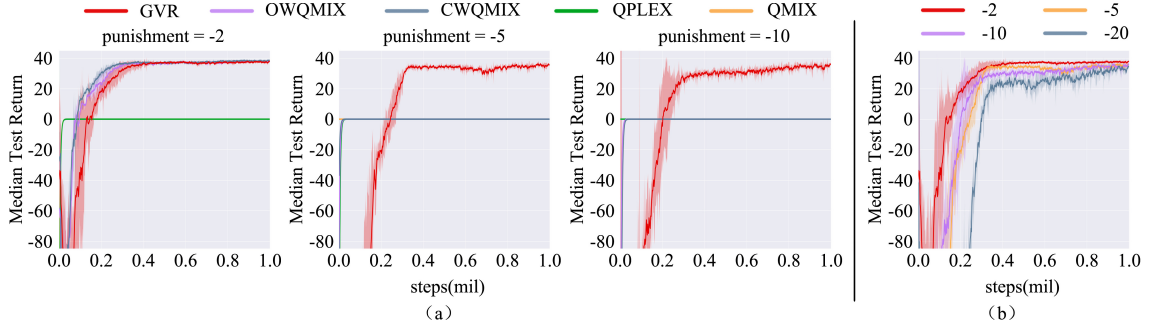


Figure 4: Experiment results on predator-prey. (a) Comparison between GVR and baselines. (b) Performance of GVR with different punishments.

5.3 STARCRAFT MULTI-AGENT CHALLENGE

StarCraft multi-agent challenge (SMAC) is a popular benchmark for the evaluation of MARL algorithms. We compare GVR with baselines in various difficult tasks of SMAC. The game version is 69232. Each algorithm is trained for 2e6 steps in MMM2, 2c_vs_64_zg and 6h_vs_8z, with ϵ damping from 1 to 0.05 during the first 5e4 steps. Especially, in 6h_vs_8z, each algorithm is trained for 5e6 steps, with ϵ damping from 1 to 0.05 during the first 1e6 steps.

From Fig.5, GVR shows the best performance. Different from predator-prey with abnormal punishments, the reward function in SMAC is more reasonable, where the linear and monotonic value decomposition can meet the TGM principle approximately. As a result, the algorithms with full representation expressiveness

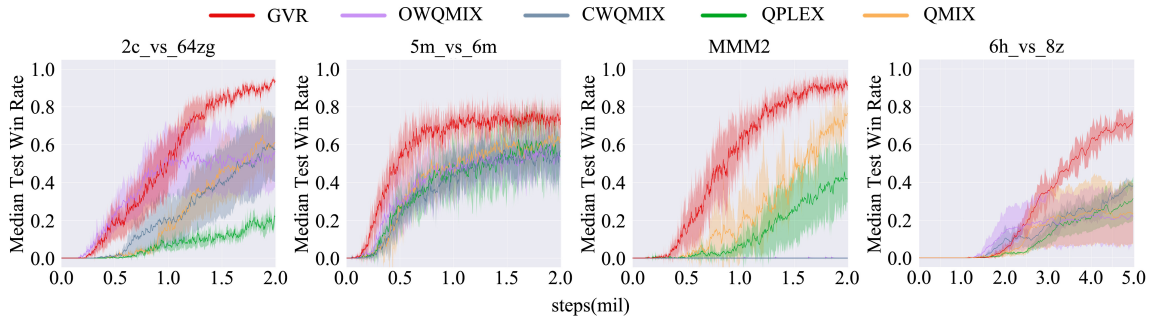


Figure 5: Median test win rate vs training steps.

capacity (QPlex, OWQMIX, CWQMIX) do not perform better than QMIX due to the difficulty of complete expressiveness.

6 CONCLUSION AND FUTURE WORK

This paper discusses the optimal coordination in fully cooperative MARL tasks and proposes a new criterion (i.e., optimal consistency) to evaluate the optimality of coordination in value decomposition. To achieve the optimal consistency, we introduce the TGM principle for linear and monotonic value decomposition and derive the general expression of the joint Q value function. We prove that the TGM principle can be ensured if the optimal stable point is the unique stable point. Therefore, we propose a quantified condition which ensures the optimal stable points and eliminates the non-optimal stable points.

To solve the problem, we propose the GVR algorithm, which is theoretically proved to ensure the optimal consistency under sufficient exploration. In experiments on matrix games, we verify our conclusions and demonstrates the effect of GVR. Besides, in experiments on predator-prey and SMAC, GVR outperforms state-of-the-art baselines. However, GVR is unable to ensure the optimal coordination in hard exploration tasks, where the superior samples are difficult to obtain and the true Q values are inaccurate. We are interested in the combination of GVR with efficient exploration approaches in future work. More discussion about the limitation of GVR is provided in Appendix L.

REFERENCES

- Wendelin Böhmer, Vitaly Kurin, and Shimon Whiteson. Deep coordination graphs. In *International Conference on Machine Learning*, pp. 980–991. PMLR, 2020.
- Jakob Foerster, Gregory Farquhar, Triantafyllos Afouras, Nantas Nardelli, and Shimon Whiteson. Counterfactual multi-agent policy gradients. In *Proceedings of the AAAI Conference on Artificial Intelligence*, volume 32, 2018.
- Jakob N Foerster, Yannis M Assael, Nando De Freitas, and Shimon Whiteson. Learning to communicate with deep multi-agent reinforcement learning. *arXiv preprint arXiv:1605.06676*, 2016.
- Carlos Guestrin, Daphne Koller, and Ronald Parr. Multiagent planning with factored mdps. In *NIPS*, volume 1, pp. 1523–1530, 2001.

-
- Tarun Gupta, Anuj Mahajan, Bei Peng, Wendelin Böhmer, and Shimon Whiteson. Uneven: Universal value exploration for multi-agent reinforcement learning. In *International Conference on Machine Learning*, pp. 3930–3941. PMLR, 2021.
- Ryan Lowe, Yi Wu, Aviv Tamar, Jean Harb, Pieter Abbeel, and Igor Mordatch. Multi-agent actor-critic for mixed cooperative-competitive environments. *arXiv preprint arXiv:1706.02275*, 2017.
- Anuj Mahajan, Tabish Rashid, Mikayel Samvelyan, and Shimon Whiteson. Maven: Multi-agent variational exploration. *arXiv preprint arXiv:1910.07483*, 2019.
- Frans A Oliehoek and Christopher Amato. *A concise introduction to decentralized POMDPs*. Springer, 2016.
- Frans A Oliehoek, Matthijs TJ Spaan, and Nikos Vlassis. Optimal and approximate q-value functions for decentralized pomdps. *Journal of Artificial Intelligence Research*, 32:289–353, 2008.
- Liviu Panait, Sean Luke, and R Paul Wiegand. Biasing coevolutionary search for optimal multiagent behaviors. *IEEE Transactions on Evolutionary Computation*, 10(6):629–645, 2006.
- Tabish Rashid, Mikayel Samvelyan, Christian Schroeder, Gregory Farquhar, Jakob Foerster, and Shimon Whiteson. Qmix: Monotonic value function factorisation for deep multi-agent reinforcement learning. In *International Conference on Machine Learning*, pp. 4295–4304. PMLR, 2018.
- Tabish Rashid, Gregory Farquhar, Bei Peng, and Shimon Whiteson. Weighted qmix: Expanding monotonic value function factorisation for deep multi-agent reinforcement learning. *arXiv preprint arXiv:2006.10800*, 2020.
- Mikayel Samvelyan, Tabish Rashid, Christian Schroeder De Witt, Gregory Farquhar, Nantas Nardelli, Tim GJ Rudner, Chia-Man Hung, Philip HS Torr, Jakob Foerster, and Shimon Whiteson. The starcraft multi-agent challenge. *arXiv preprint arXiv:1902.04043*, 2019.
- Tom Schaul, John Quan, Ioannis Antonoglou, and David Silver. Prioritized experience replay. *arXiv preprint arXiv:1511.05952*, 2015.
- Kyunghwan Son, Daewoo Kim, Wan Ju Kang, David Earl Hostallero, and Yung Yi. Qtran: Learning to factorize with transformation for cooperative multi-agent reinforcement learning. In *International Conference on Machine Learning*, pp. 5887–5896. PMLR, 2019.
- Peter Sunehag, Guy Lever, Audrunas Gruslys, Wojciech Marian Czarnecki, Vinicius Zambaldi, Max Jaderberg, Marc Lanctot, Nicolas Sonnerat, Joel Z Leibo, Karl Tuyls, et al. Value-decomposition networks for cooperative multi-agent learning. *arXiv preprint arXiv:1706.05296*, 2017.
- Sergey Vorotnikov, Konstantin Ermishin, Anaid Nazarova, and Arkady Yuschenko. Multi-agent robotic systems in collaborative robotics. In *International Conference on Interactive Collaborative Robotics*, pp. 270–279. Springer, 2018.
- Jianhao Wang, Zhizhou Ren, Terry Liu, Yang Yu, and Chongjie Zhang. Qplex: Duplex dueling multi-agent q-learning. *arXiv preprint arXiv:2008.01062*, 2020.
- Ermo Wei, Drew Wicke, David Freelan, and Sean Luke. Multiagent soft q-learning. In *2018 AAAI Spring Symposium Series*, 2018.
- Chao Wen, Xinghu Yao, Yuhui Wang, and Xiaoyang Tan. Smix (λ): Enhancing centralized value functions for cooperative multi-agent reinforcement learning. In *Proceedings of the AAAI Conference on Artificial Intelligence*, volume 34, pp. 7301–7308, 2020.

monotonic constraint is applied between the joint Q value function and individual utility functions, leading to the representation limitation of the joint Q value function. The representation limitation may result in poor credit assignment, which further introduces relative overgeneralization.

B.2 VALUE DECOMPOSITION METHODS

We mainly introduce recent value based MARL works with CTDE paradigm. Value decomposition is a popular approach for credit assignment in fully cooperative MARL methods with CTDE paradigm. VDN (Sunehag et al., 2017) learns a joint Q value function based on a share reward function. In VDN, where the joint Q value function is linearly factorized into individual utility functions. By contrast, QMIX (Rashid et al., 2018) substitutes the linear factorization with a monotonic factorization, where the weights and bias are produced from the global state through a mixing network. Based on QMIX, SMIX (Wen et al., 2020) replaces the TD(0) Q-learning target with a TD(λ) SARSA target. Qatten (Yang et al., 2020b) adds an attention network before the mixing network of QMIX. QPD (Yang et al., 2020a) decomposes the joint Q value function with the integrated gradient attribution technique, which directly decomposes the joint Q-values along trajectory paths to assign credits for agents. However, due to the representation limitation of the joint Q value function, these methods suffer from the relative overgeneralization. As a result, they can not guarantee the optimal coordination.

Some of recent works try to solve the representation limitation directly through joint Q value function with complete expressiveness capacity. QTRAN learns a joint Q value function with complete expressiveness capacity and introduces two soft regularizations to approximate the IGM principle. QPLEX (Wang et al., 2020) achieves the complete expressive under IGM principle theoretically through a dueling mixing network, where the complete expressiveness capacity is introduced by the mixing of individual advantage functions. However, as the state space and the joint action space increase exponentially as the number of agents grows, it is impractical to learn the complete expressiveness in complicated MARL tasks, which may result in convergence difficulty and performance deterioration.

The other works improve the coordination from different perspectives. WQMIX (Rashid et al., 2020) tries to solve the underestimation of the optimal joint values that arise from the representation limitation, where an auxiliary network with complete expressiveness capacity is applied to distinguishes samples with low expressive values. By placing a predefined weight on these samples, WQMIX can alleviate the underestimation of optimal joint Q values. According to Appendix G, a relative higher weight on the superior samples helps to eliminate non-optimal stable points. Therefore, WQMIX is effective to overcome relative overgeneralization to some degree, which is verified by our experiments on predator-prey. However, the joint Q value function under monotonic factorization depends heavily on the reward function, which is unavailable and task-specific. As a result, a heuristic weight has to be adopted in WQMIX, which can not guarantee the optimal coordination.

MAVEN (Mahajan et al., 2019) focuses on the poor exploration that arises from the representation limitation and introduces a latent space for hierarchical control, which achieves temporally extended exploration. UneVEN (Gupta et al., 2021) solves the target task by learning a set of related tasks simultaneously with a linear decomposition of universal successor features, which improves the joint exploration. Both methods raise the proportion of superior samples through an improved joint exploration, which helps to eliminate non-optimal stable points according to Eq.8. However, it requires an enormous exploration to raise the proportion of superior samples under large joint action space, which may reduce the sample efficiency. In practice, both methods apply small noise for joint exploration, where the proportion of superior samples increases slightly. As a result, both methods are insufficient to ensure the optimal coordination.

related works	IGM principle	TGM principle
IQL	No	No
VDN	Yes	No
QMIX	Yes	No
SMIX	Yes	No
Qatten	Yes	No
QDP	No	No
QTRAN	No	Yes
MAVEN	Yes	No
UneVEn	Yes	No
WQMIX	Yes	No
QPLEX	Yes	Yes
GVR(ours)	Yes	Yes

Table 1: Whether related works ensure the IGM and TGM principle.

C JOINT Q VALUES REPRESENTED BY TRUE Q VALUES FOR TWO-AGENT LINEAR VALUE DECOMPOSITION

C.1 DERIVATION

Consider a two-agent fully cooperative task without experience replay. the joint Q value function $Q(u_i^1, u_j^2, \tau)$ is linearly factorized into two utility functions $\mathcal{U}^1(u_i^1, \tau^1)$ and $\mathcal{U}^2(u_j^2, \tau^2)$.

$$Q(u_i^1, u_j^2, \tau) = \mathcal{U}^1(u_i^1, \tau^1) + \mathcal{U}^2(u_j^2, \tau^2) \quad (13)$$

where $u_i^1, u_j^2 \in \{u_1, \dots, u_m\}$ denote the individual actions of agent 1,2 respectively. $\{u_1, \dots, u_m\}$ is the discrete individual action space. Specially, we denote the individual greedy action of agent 1,2 with \hat{u}_i^1, \hat{u}_j^2 respectively. For briefness, we denote $Q(u_i^1, u_j^2, \tau)$, $\mathcal{U}^a(u_i^a, \tau^a)$ with Q_{ij} , \mathcal{U}_i^a ($a \in \{1, 2\}$) respectively. Under ϵ -greedy visitation, we have

$$\begin{aligned} \mathcal{U}_i^1 &= \frac{\epsilon}{m} \sum_{k=1}^m (\mathcal{Q}_{ik} - \mathcal{U}_k^2) + (1 - \epsilon)(\mathcal{Q}_{i\hat{j}} - \mathcal{U}_{\hat{j}}^2) \\ \mathcal{U}_j^2 &= \frac{\epsilon}{m} \sum_{k=1}^m (\mathcal{Q}_{kj} - \mathcal{U}_k^1) + (1 - \epsilon)(\mathcal{Q}_{i\hat{j}} - \mathcal{U}_i^1) \end{aligned} \quad (14)$$

where \mathcal{Q}_{ij} is the true Q value. The sum of two utility functions over all actions equals to

$$\begin{aligned} \sum_{i=1}^m \mathcal{U}_i^1 + \sum_{j=1}^m \mathcal{U}_j^2 &= \frac{\epsilon}{m} \left[\sum_{i=1}^m \sum_{k=1}^m \mathcal{Q}_{ik} + \sum_{j=1}^m \sum_{k=1}^m \mathcal{Q}_{kj} - m \sum_{k=1}^m (\mathcal{U}_k^1 + \mathcal{U}_k^2) \right] \\ &\quad + (1 - \epsilon) \left[\sum_{i=1}^m (\mathcal{Q}_{i\hat{j}} + \mathcal{Q}_{i\hat{j}}) - m(\mathcal{U}_i^1 + \mathcal{U}_{\hat{j}}^2) \right] \end{aligned} \quad (15)$$

Notice that $\mathcal{U}_i^1 + \mathcal{U}_{\hat{j}}^2 = \mathcal{Q}_{i\hat{j}}$, and $\sum_{i=1}^m \sum_{k=1}^m \mathcal{Q}_{ik} = \sum_{j=1}^m \sum_{k=1}^m \mathcal{Q}_{kj} = \sum_{i=1}^m \sum_{j=1}^m \mathcal{Q}_{ij}$, we have

$$\sum_{k=1}^m (\mathcal{U}_k^1 + \mathcal{U}_k^2) = \frac{2\epsilon}{m(1 + \epsilon)} \sum_{i=1}^m \sum_{j=1}^m \mathcal{Q}_{ij} + \frac{1 - \epsilon}{1 + \epsilon} \sum_{k=1}^m (\mathcal{Q}_{ik} + \mathcal{Q}_{k\hat{j}}) - \frac{m(1 - \epsilon)}{1 + \epsilon} \mathcal{Q}_{i\hat{j}} \quad (16)$$

According to Eq.14 and Eq.16, for $\forall i, j \in [1, m]$, the joint Q value function equals to

$$\begin{aligned}
Q_{ij} &= \mathcal{U}_i^1 + \mathcal{U}_j^2 \\
&= \frac{\epsilon}{m} \left[\sum_{k=1}^m (\mathcal{Q}_{ik} + \mathcal{Q}_{kj}) - \sum_{k=1}^m (\mathcal{U}_k^1 + \mathcal{U}_k^2) \right] + (1 - \epsilon)(\mathcal{Q}_{ij} + \mathcal{Q}_{ij} - \mathcal{Q}_{ij}) \\
&= \frac{\epsilon}{m} \sum_{k=1}^m (\mathcal{Q}_{ik} + \mathcal{Q}_{kj}) + (1 - \epsilon)(\mathcal{Q}_{ij} + \mathcal{Q}_{ij}) - \frac{2\epsilon^2}{m^2(1 + \epsilon)} \sum_{i=1}^m \sum_{j=1}^m \mathcal{Q}_{ij} - \frac{1 - \epsilon}{1 + \epsilon} \mathcal{Q}_{ij} \\
&\quad - \frac{\epsilon(1 - \epsilon)}{m(1 + \epsilon)} \sum_{k=1}^m (\mathcal{Q}_{ik} + \mathcal{Q}_{kj})
\end{aligned} \tag{17}$$

Notice that Q_{ij} is related to the joint greedy Q value Q_{ij} . In order to remove it, we put i and j into Eq.17.

$$Q_{ij} = \frac{\epsilon^2}{m} \sum_{k=1}^m (\mathcal{Q}_{ik} + \mathcal{Q}_{kj}) - \frac{\epsilon^2}{m^2} \sum_{i=1}^m \sum_{j=1}^m \mathcal{Q}_{ij} + (1 - \epsilon^2) \mathcal{Q}_{ij} \tag{18}$$

Substituting Eq.18 into Eq.17, the joint Q values can be represented by true Q values as

$$\begin{aligned}
Q_{ij} &= \frac{\epsilon}{m} \sum_{k=1}^m (\mathcal{Q}_{ik} + \mathcal{Q}_{kj}) + (1 - \epsilon)(\mathcal{Q}_{ij} + \mathcal{Q}_{ij}) - \frac{\epsilon^2}{m^2} \sum_{i=1}^m \sum_{j=1}^m \mathcal{Q}_{ij} \\
&\quad - \frac{\epsilon(1 - \epsilon)}{m} \sum_{k=1}^m (\mathcal{Q}_{ik} + \mathcal{Q}_{kj}) - (1 - \epsilon)^2 \mathcal{Q}_{ij}
\end{aligned} \tag{19}$$

C.2 VERIFICATION

We verify the expression of Eq.19 in a two-agent matrix game, where the payoff matrix is shown in Table2(a). Since the episode length is 1, an mlp shared by two agents is adopted as the policy network. The policy network is trained for 200 iterations (100 episodes per iteration) over 5 seeds. According to Table2(b) and 2(c). There are two stable points, which consists with our calculation. The error of joint Q values between calculation and test is lower than 3%.

8	-12	-12
-12	0	0
-12	0	6

(a)

7.40 (7.38±0.02)	-8.33 (-8.27±0.12)	-7.93 (-7.86±0.13)
-8.33 (-8.33±0.18)	-24.06 (-23.87±0.09)	-23.66 (-23.56±0.17)
-7.93 (-7.93±0.09)	-23.66 (-23.53±0.12)	-23.26 (-23.19±0.20)

(b)

-24.38 (-24.34±0.25)	-14.52 (-14.52±0.11)	-9.32 (-9.43±0.15)
-14.52 (-14.47±0.18)	-4.65 (-4.65±0.11)	0.55 (0.54±0.08)
-9.32 (-9.28±0.21)	0.55 (0.56±0.12)	5.75 (5.75±0.09)

(c)

Table 2: Verification of calculated stable points for two-agent LVD. (a) The payoff matrix. (b),(c) Comparison between calculation and test, where the test results are shown in parentheses. The numbers in bold denote the max joint Q values, and the greedy policy is marked with a pink background.

D JOINT Q VALUES REPRESENTED BY TRUE Q VALUES FOR TWO-AGENT MONOTONIC VALUE DECOMPOSITION

For two-agent monotonic value decomposition, the joint Q value function is decomposed as $Q_{ij} = \omega_1(s)\mathcal{U}_i^1 + \omega_2(s)\mathcal{U}_j^2 + V(s)$, where ω_1 and ω_2 are the coefficients of \mathcal{U}_i^1 and \mathcal{U}_j^2 respectively. $V(s)$ is the bias, which is the same for all joint actions under a given state. For brevity, we omit the input. Referring to Eq.14, the individual utility functions with coefficients equal to

$$\begin{aligned}\omega_1\mathcal{U}_i^1 &= \frac{\epsilon}{m} \sum_{k=1}^m [\mathcal{Q}_{ik} - \omega_2\mathcal{U}_k^2 - V] + (1-\epsilon) [\mathcal{Q}_{i\dot{j}} - \omega_2\mathcal{U}_{\dot{j}}^2 - V] \\ &= \frac{\epsilon}{m} \sum_{k=1}^m [\mathcal{Q}_{ik} - \omega_2\mathcal{U}_k^2] + (1-\epsilon) [\mathcal{Q}_{i\dot{j}} - \omega_2\mathcal{U}_{\dot{j}}^2] - V \\ \omega_2\mathcal{U}_j^2 &= \frac{\epsilon}{m} \sum_{k=1}^m [\mathcal{Q}_{kj} - \omega_1\mathcal{U}_k^1 - V] + (1-\epsilon) [\mathcal{Q}_{i\dot{j}} - \omega_1\mathcal{U}_{\dot{i}}^1 - V] \\ &= \frac{\epsilon}{m} \sum_{k=1}^m [\mathcal{Q}_{ik} - \omega_2\mathcal{U}_k^2] + (1-\epsilon) [\mathcal{Q}_{i\dot{j}} - \omega_2\mathcal{U}_{\dot{j}}^2] - V\end{aligned}\tag{20}$$

Referring to the derivation of Eq.16, we have

$$\sum_{k=1}^m (\omega_1\mathcal{U}_k^1 + \omega_2\mathcal{U}_k^2) = \frac{2\epsilon}{m(1+\epsilon)} \sum_{i=1}^m \sum_{j=1}^m \mathcal{Q}_{ij} + \frac{1-\epsilon}{1+\epsilon} \sum_{k=1}^m (\mathcal{Q}_{ik} + \mathcal{Q}_{k\dot{j}}) - \frac{m(1-\epsilon)}{1+\epsilon} \mathcal{Q}_{i\dot{j}} - mV\tag{21}$$

According to Eq.20 and Eq.21, we have

$$\begin{aligned}\mathcal{Q}_{ij} &= \frac{\epsilon}{m} \sum_{k=1}^m (\mathcal{Q}_{ik} + \mathcal{Q}_{kj}) + (1-\epsilon)(\mathcal{Q}_{i\dot{j}} + \mathcal{Q}_{\dot{i}j}) - \frac{2\epsilon^2}{m^2(1+\epsilon)} \sum_{i=1}^m \sum_{j=1}^m \mathcal{Q}_{ij} \\ &\quad - \frac{1-\epsilon}{1+\epsilon} \mathcal{Q}_{i\dot{j}} - \frac{\epsilon(1-\epsilon)}{m(1+\epsilon)} \sum_{k=1}^m (\mathcal{Q}_{ik} + \mathcal{Q}_{k\dot{j}})\end{aligned}\tag{22}$$

In order to remove $\mathcal{Q}_{i\dot{j}}$ from Eq.22, let $i = \dot{i}$ and $j = \dot{j}$.

$$\mathcal{Q}_{i\dot{j}} = \frac{\epsilon^2}{m} \sum_{k=1}^m (\mathcal{Q}_{ik} + \mathcal{Q}_{k\dot{j}}) - \frac{\epsilon^2}{m^2} \sum_{i=1}^m \sum_{j=1}^m \mathcal{Q}_{ij} + (1-\epsilon^2)\mathcal{Q}_{i\dot{j}}\tag{23}$$

Substituting Eq.23 into Eq.22, we have

$$\begin{aligned}\mathcal{Q}_{ij} &= \frac{\epsilon}{m} \sum_{k=1}^m (\mathcal{Q}_{ik} + \mathcal{Q}_{kj}) + (1-\epsilon)(\mathcal{Q}_{i\dot{j}} + \mathcal{Q}_{\dot{i}j}) - \frac{\epsilon^2}{m^2} \sum_{i=1}^m \sum_{j=1}^m \mathcal{Q}_{ij} \\ &\quad - \frac{\epsilon(1-\epsilon)}{m} \sum_{k=1}^m (\mathcal{Q}_{ik} + \mathcal{Q}_{k\dot{j}}) - (1-\epsilon)^2 \mathcal{Q}_{i\dot{j}}\end{aligned}\tag{24}$$

E EXPLANATIONS OF REMARK 1.

To explain the condition (Eq.5, section 3.2) in Remark 1, consider two cases.

(1) Suppose $\hat{\mathbf{u}}$ is the optimal action, i.e., $\hat{\mathbf{u}} = \operatorname{argmax}_{\mathbf{u}} \pi(\mathbf{u}|\tau) = \mathbf{u}^*$, we have $\Delta Q(s, \mathbf{u}_s) \leq 0$. According to Eq.5 (in section 3.2), $\Delta Q(\mathbf{u}_s, \tau) < 0$ for $\forall \mathbf{u}_s \neq \mathbf{u}^*$. By Def.3 in section 3.2, the optimal point is stable since $\operatorname{argmax}_{\mathbf{u}} Q(\mathbf{u}, \tau) = \mathbf{u}^* = \operatorname{argmax}_{\mathbf{u}} \pi(\mathbf{u}|\tau)$. An example of this case is shown in Fig.7(a).

(2) Suppose $\hat{\mathbf{u}}$ is not the optimal action, $\exists \mathbf{u}_s$ such that $\Delta Q(s, \mathbf{u}_s) > 0$. According to Eq.5 in section 3.2, $\Delta Q(\mathbf{u}_s, \tau) > 0$ for such \mathbf{u}_s . By Def.3 in section 3.2, the non-optimal point is unstable since $\operatorname{argmax}_{\mathbf{u}} Q(\mathbf{u}, \tau) \neq \hat{\mathbf{u}} = \operatorname{argmax}_{\mathbf{u}} \pi(\mathbf{u}|\tau)$. Examples of this case are shown in Fig.7(b)(c).

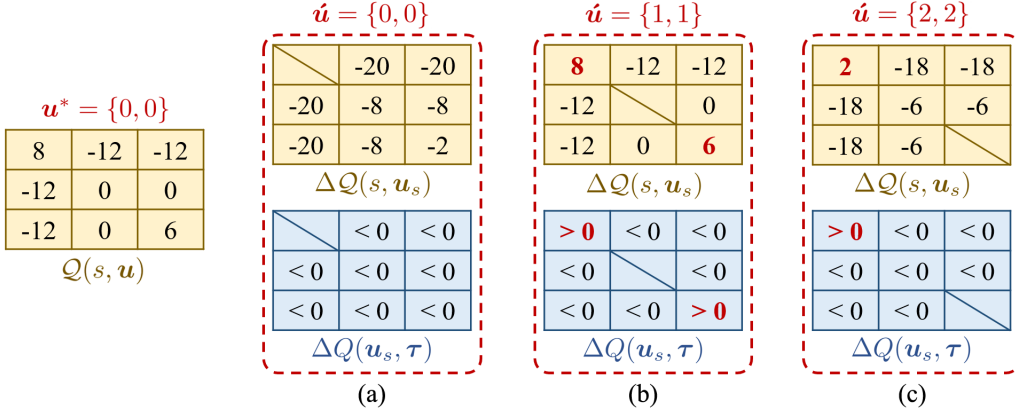


Figure 7: An example satisfying the condition (Eq.5, section 3.2) in Remark 1, where $\mathbf{u}_s \neq \hat{\mathbf{u}}$, $\Delta Q(s, \mathbf{u}_s) = Q(s, \mathbf{u}_s) - Q(s, \hat{\mathbf{u}})$, and $\Delta Q(\mathbf{u}_s, \tau) = Q(\mathbf{u}_s, \tau) - Q(\hat{\mathbf{u}}, \tau)$.

F STABLE POINTS UNDER ITS

F.1 PROOF 1

Given the greedy action $\hat{\mathbf{u}} = \{\hat{u}^1, \dots, \hat{u}^n\}$ and any action $\mathbf{u}_s = \{u_s^1, \dots, u_s^n\}$ ($\mathbf{u}_s \neq \hat{\mathbf{u}}$), assuming $Q(s, \hat{\mathbf{u}}) > 0$ (i.e. $Q_{its}(s, \mathbf{u}) = (1 - \alpha)Q(\hat{\mathbf{u}}, \tau)$ for inferior samples), under the hardest exploration case where $u_s^a \neq \hat{u}^a (\forall a \in [1, n])$, the utility function of individual action $u_s^a (a \in [1, n])$ is consist of two parts

$$\begin{aligned} \mathcal{U}^a(u_s^a, \tau^a) = & (1 - \eta_1) \left[(1 - \alpha)Q(\hat{\mathbf{u}}, \tau) - \sum_k^{m^{n-1}-1} \left[\frac{p(u_s^a, u_k^{-a})}{p(u_s^a) - p(\mathbf{u}_s)} \sum_i^{-a} \mathcal{U}^i(u_k^i, \tau^i) \right] \right] \\ & + \eta_1 \left[Q_{its}(s, \mathbf{u}_s) - \sum_i^{-a} \mathcal{U}^i(u_s^i, \tau^i) \right] \end{aligned} \quad (25)$$

where $\eta_1 = (\frac{\epsilon}{m})^{n-1}$, and $-a$ represents the collection of all agents expect agent a . η_1 and $1 - \eta_1$ are the proportion (in all samples containing u_s^a) of sample \mathbf{u}_s and inferior samples respectively. $\sum_k^{m^{n-1}} \{u_s^a, u_k^{-a}\}$ is the collection of all samples containing u_s^a , and $p(u_s^a, u_k^{-a})$ is the corresponding probability of each sample. Notice the superscript of the first \sum in Eq.25 is $m^{n-1} - 1$, where the sample \mathbf{u}_s is excluded.

$p(u_s^a) - p(\mathbf{u}_s) = \sum_k^{m^{n-1}} p(u_s^a, u_k^{-a}) = \frac{\epsilon}{m} - (\frac{\epsilon}{m})^n$ is the normalization coefficient. We ignore the other potential superior samples. Notice

$$\begin{aligned} (1 - \eta_1) \sum_k^{m^{n-1}-1} \left[\frac{p(u_s^a, u_k^{-a})}{p(u_s^a) - p(\mathbf{u}_s)} \sum_i^{-a} \mathcal{U}^i(u_k^i, \tau^i) \right] + \eta_1 \sum_i^{-a} \mathcal{U}^i(u_k^i, \tau^i) \\ = \sum_k^{m^{n-1}} \left[\frac{p(u_s^a, u_k^{-a})}{p(u_s^a)} \sum_i^{-a} \mathcal{U}^i(u_k^i, \tau^i) \right] \end{aligned} \quad (26)$$

Therefore,

$$\mathcal{U}^a(u_s^a, \tau^a) = (1 - \eta_1)(1 - \alpha)Q(\mathbf{u}, \tau) - \sum_k^{m^{n-1}} \left[\frac{p(u_s^a, u_k^{-a})}{p(u_s^a)} \sum_i^{-a} \mathcal{U}^i(u_k^i, \tau^i) \right] + \eta_1 \mathcal{Q}_{its}(s, \mathbf{u}_s) \quad (27)$$

The joint Q value function $Q(\mathbf{u}_s, \tau)$ can be acquired

$$\begin{aligned} Q(\mathbf{u}_s, \tau) &= \sum_{a=1}^n \mathcal{U}^a(u_s^a, \tau^a) \\ &= n(1 - \eta_1)(1 - \alpha)Q(\mathbf{u}, \tau) - \sum_{a=1}^n \sum_k^{m^{n-1}} \left[\frac{p(u_s^a, u_k^{-a})}{p(u_s^a)} \sum_i^{-a} \mathcal{U}^i(u_k^i, \tau^i) \right] + n\eta_1 \mathcal{Q}_{its}(s, \mathbf{u}_s) \end{aligned} \quad (28)$$

Similarly, for the greedy action \mathbf{u} , we have

$$\mathcal{U}^a(\mathbf{u}^a, \tau^a) = (1 - \eta_2)(1 - \alpha)Q(\mathbf{u}, \tau) - \sum_k^{m^{n-1}} \left[\frac{p(\mathbf{u}^a, u_k^{-a})}{p(\mathbf{u}^a)} \sum_i^{-a} \mathcal{U}^i(u_k^i, \tau^i) \right] + \eta_2 \mathcal{Q}(s, \mathbf{u}) \quad (29)$$

where $\eta_2 = (1 - \epsilon + \frac{\epsilon}{m})^{n-1}$. As a result,

$$\begin{aligned} Q(\mathbf{u}, \tau) &= \sum_{a=1}^n \mathcal{U}^a(\mathbf{u}^a, \tau^a) \\ &= n(1 - \eta_2)(1 - \alpha)Q(\mathbf{u}, \tau) - \sum_{a=1}^n \sum_k^{m^{n-1}} \left[\frac{p(\mathbf{u}^a, u_k^{-a})}{p(\mathbf{u}^a)} \sum_i^{-a} \mathcal{U}^i(u_k^i, \tau^i) \right] + n\eta_2 \mathcal{Q}(s, \mathbf{u}) \end{aligned} \quad (30)$$

Notice $\frac{p(u_s^a, u_k^{-a})}{p(u_s^a)}$ is independent to action u^a for decentralized execution, therefore $\frac{p(\mathbf{u}^a, u_k^{-a})}{p(\mathbf{u}^a)} = \frac{p(u_s^a, u_k^{-a})}{p(u_s^a)}$. Let $\mathcal{Q}(s, \mathbf{u}_s) = (1 + e_Q)\mathcal{Q}(s, \mathbf{u})$, according to Eq.28 and Eq.30, we have

$$\Delta Q(\mathbf{u}_s, \tau) = Q(\mathbf{u}_s, \tau) - Q(\mathbf{u}, \tau) = n(\eta_1 - \eta_2) [\mathcal{Q}(s, \mathbf{u}^*) - (1 - \alpha)Q(\mathbf{u}, \tau)] + n\eta_1 e_Q \mathcal{Q}(s, \mathbf{u}) \quad (31)$$

For monotonic value decomposition, Eq.37 also holds since the expressions of $Q(\mathbf{u}, \tau)$ and $Q(\mathbf{u}_s, \tau)$ do not change. Verification of Eq.31 is provided in the experimental part of the main body.

Since $Q(\mathbf{u}, \tau)$ is an expectation of $\mathcal{Q}(s, \mathbf{u})$, for $\forall \mathbf{u} \in U^n$, $Q(\mathbf{u}, \tau) < \max \mathcal{Q}(s, \mathbf{u})$ holds. If the \mathbf{u} is exact the optimal action, i.e., $\mathbf{u} = \arg\max_{\mathbf{u}} \mathcal{Q}(s, \mathbf{u})$, for $\forall \mathbf{u}_s \in U^n$, $e_Q < 0$ and $Q(\mathbf{u}, \tau) - \mathcal{Q}(s, \mathbf{u}) < 0$ hold. Therefore, for $\forall \mathbf{u}_s \in U^n$, $\Delta Q(\mathbf{u}_s, \tau) < 0$ holds, which indicate when the greedy action is the optimal action,

the joint Q value of the optimal action is the maximal, i.e., **there is always an optimal stable point under ITS.**

If $\hat{\mathbf{u}}$ is a non-optimal action, to destabilize it, let $\Delta Q(\mathbf{u}_s, \tau) > 0$ and assume $Q(\hat{\mathbf{u}}, \tau) \approx Q(s, \hat{\mathbf{u}})$ (this assumption is quite accurate, as verified in Appendix G.2), we have

$$\frac{\eta_1}{\eta_2} > \frac{\alpha}{\alpha + e_Q} \quad (32)$$

which indicates the non-optimal stable points can be eliminated by raising $\frac{\eta_1}{\eta_2}$ under ITS.

F.2 PROOF 2

Given the greedy action $\hat{\mathbf{u}} = \{\hat{u}^1, \dots, \hat{u}^n\}$ and any action $\mathbf{u}_s = \{u_s^1, \dots, u_s^n\} (\mathbf{u}_s \neq \hat{\mathbf{u}})$, assuming $Q(s, \hat{\mathbf{u}}) > 0$ (i.e. $Q_{its}(s, \mathbf{u}) = (1 - \alpha)Q(\hat{\mathbf{u}}, \tau)$ for inferior samples), under the hardest exploration case where $u_s^a \neq \hat{u}^a (\forall a \in [1, n])$, the utility function of u_s^a equals to

$$\begin{aligned} \mathcal{U}_{u_s^a}^a &= \left(\frac{\epsilon}{m}\right)^{n-1} \left[C_{n-1}^0 (m^{n-1} - 1)(1 - \alpha)Q(\hat{\mathbf{u}}, \tau) + Q(s, \mathbf{u}_s) + f_1\left(\sum_o^{-a} \sum_{i=1}^m \mathcal{U}_{u_i^o}^o, \sum_{a=1}^n \mathcal{U}_{\hat{u}^a}^a\right) \right] \\ &+ \dots + \left(\frac{\epsilon}{m}\right)^{n-t} (1 - \epsilon)^{t-1} \left[C_{n-1}^{t-1} m^{n-t} (1 - \alpha)Q(\hat{\mathbf{u}}, \tau) + f_t\left(\sum_o^{-a} \sum_{i=1}^m \mathcal{U}_{u_i^o}^o, \sum_{a=1}^n \mathcal{U}_{\hat{u}^a}^a\right) \right] + \dots \\ &+ (1 - \epsilon)^{n-1} \left[C_{n-1}^{n-1} (1 - \alpha)Q(\hat{\mathbf{u}}, \tau) + f_n\left(\sum_o^{-a} \sum_{i=1}^m \mathcal{U}_{u_i^o}^o, \sum_{a=1}^n \mathcal{U}_{\hat{u}^a}^a\right) \right] \\ &= (1 - \alpha)Q(\hat{\mathbf{u}}, \tau) + \left(\frac{\epsilon}{m}\right)^{n-1} [Q(s, \mathbf{u}_s) - (1 - \alpha)Q(\hat{\mathbf{u}}, \tau)] + f_{total}\left(\sum_o^{-a} \sum_{i=1}^m \mathcal{U}_{u_i^o}^o, \sum_{a=1}^n \mathcal{U}_{\hat{u}^a}^a\right) \end{aligned} \quad (33)$$

where $-a$ represents the collection of all agents except agent a . $f_t (t \in [1, n])$ and f_{total} are mappings from $\{\sum_o^{-a} \sum_{i=1}^m \mathcal{U}_{u_i^o}^o, \sum_{a=1}^n \mathcal{U}_{\hat{u}^a}^a\}$ to \mathbb{R} . We ignore the other potential superior samples. The joint Q value function of \mathbf{u}_s equals to

$$\begin{aligned} Q(\mathbf{u}_s, \tau) &= \sum_{a=1}^n \mathcal{U}_{u_s^a}^a \\ &= n(1 - \alpha)Q(\hat{\mathbf{u}}, \tau) + n \left(\frac{\epsilon}{m}\right)^{n-1} [Q(s, \mathbf{u}_s) - (1 - \alpha)Q(\hat{\mathbf{u}}, \tau)] + n f_{total}\left(\sum_o^{-a} \sum_{i=1}^m \mathcal{U}_{u_i^o}^o, \sum_{a=1}^n \mathcal{U}_{\hat{u}^a}^a\right) \end{aligned} \quad (34)$$

Next we calculate the joint Q value of the greedy action. The utility function of the individual greedy action $\hat{u}^a (a \in [1, n])$ equals to

$$\begin{aligned} \mathcal{U}_{\hat{u}^a}^a &= (1 - \alpha)Q(\hat{\mathbf{u}}, \tau) \\ &+ (1 - \epsilon + \frac{\epsilon}{m})^{n-1} [Q(s, \hat{\mathbf{u}}) - (1 - \alpha)Q(\hat{\mathbf{u}}, \tau)] + f_{total}\left(\sum_o^{-a} \sum_{i=1}^m \mathcal{U}_{u_i^o}^o, \sum_{a=1}^n \mathcal{U}_{\hat{u}^a}^a\right) \end{aligned} \quad (35)$$

The joint Q value of greedy action equals to

$$\begin{aligned} Q(\hat{\mathbf{u}}, \tau) &= \sum_{a=1}^n \mathcal{U}_{\hat{u}^a}^a = n(1 - \alpha)Q(\hat{\mathbf{u}}, \tau) \\ &+ n(1 - \epsilon + \frac{\epsilon}{m})^{n-1} [Q(s, \hat{\mathbf{u}}) - (1 - \alpha)Q(\hat{\mathbf{u}}, \tau)] + n f_{total}\left(\sum_o^{-a} \sum_{i=1}^m \mathcal{U}_{u_i^o}^o, \sum_{a=1}^n \mathcal{U}_{\hat{u}^a}^a\right) \end{aligned} \quad (36)$$

Notice $\eta_1 = (\frac{\epsilon}{m})^{n-1}$, $\eta_2 = (1 - \epsilon + \frac{\epsilon}{m})^{n-1}$ and $\mathcal{Q}(s, \mathbf{u}_s) = (1 + e_Q)\mathcal{Q}(s, \hat{\mathbf{u}})$ according to Eq.34 and Eq.36

$$\begin{aligned}\Delta Q(\mathbf{u}_s, \boldsymbol{\tau}) &= Q(\mathbf{u}_s, \boldsymbol{\tau}) - Q(\hat{\mathbf{u}}, \boldsymbol{\tau}) \\ &= n\eta_1 [(1 + e_Q)\mathcal{Q}(s, \hat{\mathbf{u}}) - (1 - \alpha)Q(\hat{\mathbf{u}}, \boldsymbol{\tau})] - n\eta_2 [\mathcal{Q}(s, \hat{\mathbf{u}}) - (1 - \alpha)Q(\hat{\mathbf{u}}, \boldsymbol{\tau})] \\ &= n(\eta_1 - \eta_2) [\mathcal{Q}(s, \hat{\mathbf{u}}) - (1 - \alpha)Q(\hat{\mathbf{u}}, \boldsymbol{\tau})] + n\eta_1 e_Q \mathcal{Q}(s, \hat{\mathbf{u}})\end{aligned}\quad (37)$$

which consist with Eq.31 in Proof 1.

F.3 NON-HARDEST EXPLORATION CASES UNDER ITS

In Proof 1 and Proof 2, we only consider the hardest exploration case, where $u_s^a \neq \hat{u}^a (\forall a \in [1, n])$. In this subsection, we provide the proof of $\Delta Q(\mathbf{u}_s, \boldsymbol{\tau})$ in general cases where

$$u_s^a \begin{cases} = \hat{u}^a & a \in \mathcal{L} \\ \neq \hat{u}^a & \text{others} \end{cases} \quad (38)$$

$\mathcal{L} \in \{1, \dots, n\}$ and $\mathcal{L} \neq \emptyset$. Assuming $\mathcal{Q}(s, \hat{\mathbf{u}}) > 0$ (i.e. $\mathcal{Q}_{its}(s, \mathbf{u}) = (1 - \alpha)Q(\hat{\mathbf{u}}, \boldsymbol{\tau})$ for inferior samples), when $a \in \mathcal{L}$, the utility function of individual action u_s^a is consist of three parts

$$\begin{aligned}\mathcal{U}^a(u_s^a, \tau^a) &= \mathcal{U}^a(\hat{u}^a, \tau^a) = \eta'_1 \left[\mathcal{Q}_{its}(s, \mathbf{u}_s) - \sum_i^{-a} \mathcal{U}^i(u_s^i, \tau^i) \right] + \eta_2 \left[\mathcal{Q}(s, \hat{\mathbf{u}}) - \sum_i^{-a} \mathcal{U}^i(\hat{u}^i, \tau^i) \right] \\ &\quad + (1 - \eta'_1 - \eta_2) \left[(1 - \alpha)Q(\hat{\mathbf{u}}, \boldsymbol{\tau}) - \sum_k^{m^{n-1}-2} \left[\frac{p(u_s^a, u_k^{-a})}{p(u_s^a) - p(\mathbf{u}_s)} \sum_i^{-a} \mathcal{U}^i(u_k^i, \tau^i) \right] \right]\end{aligned}\quad (39)$$

where $\eta'_1 = (\frac{\epsilon}{m})^{n-l}(1 - \epsilon - \frac{\epsilon}{m})^{l-1}$, $\eta_2 = (1 - \epsilon - \frac{\epsilon}{m})^{n-1}$. When $a \notin \mathcal{L}$, according to Eq.27, we have

$$\mathcal{U}^a(u_s^a, \tau^a) = (1 - \eta'_1)(1 - \alpha)Q(\hat{\mathbf{u}}, \boldsymbol{\tau}) - \sum_k^{m^{n-1}} \left[\frac{p(u_s^a, u_k^{-a})}{p(u_s^a)} \sum_i^{-a} \mathcal{U}^i(u_k^i, \tau^i) \right] + \eta'_1 \mathcal{Q}_{its}(s, \mathbf{u}_s) \quad (40)$$

As a result,

$$\mathcal{U}^a(u_s^a, \tau^a) = \begin{cases} \text{Eq.39} & a \in \mathcal{L} \\ \text{Eq.40} & \text{others} \end{cases} \quad \mathcal{U}^a(\hat{u}^a, \tau^a) = \begin{cases} \text{Eq.39} & a \in \mathcal{L} \\ \text{Eq.29} & \text{others} \end{cases} \quad (41)$$

Therefore,

$$\begin{aligned}\Delta Q(\mathbf{u}_s, \boldsymbol{\tau}) &= Q(\mathbf{u}_s, \boldsymbol{\tau}) - Q(\hat{\mathbf{u}}, \boldsymbol{\tau}) = \sum_a^{[1, n] - \mathcal{L}} [\mathcal{U}^a(u_s^a, \tau^a) - \mathcal{U}^a(\hat{u}^a, \tau^a)] \\ &= (n - l)(\eta'_1 - \eta_2) [\mathcal{Q}(s, \hat{\mathbf{u}}) - (1 - \alpha)Q(\hat{\mathbf{u}}, \boldsymbol{\tau})] + (n - l)\eta'_1 e_Q \mathcal{Q}(s, \hat{\mathbf{u}})\end{aligned}\quad (42)$$

To eliminate non-optimal stable points, let $\Delta Q(\mathbf{u}_s, \boldsymbol{\tau}) > 0$ and assume $Q(\hat{\mathbf{u}}, \boldsymbol{\tau}) \approx \mathcal{Q}(s, \hat{\mathbf{u}})$ (this assumption is quite accurate, as verified in Appendix G.2), we have

$$\frac{\eta'_1}{\eta_2} > \frac{\alpha}{\alpha + e_Q} \quad (43)$$

which equals to

$$\left(\frac{\frac{\epsilon}{m}}{1 - \epsilon - \frac{\epsilon}{m}} \right)^{n-l} > \frac{\alpha}{\alpha + e_Q} \quad (44)$$

Since $l \geq 1$, $\frac{\eta_1}{\eta_2} > \frac{\eta'_1}{\eta_2}$, thus **Eq.44 is a sufficient condition for Eq.32.**

G LVD AND MVD UNDER ITS WITH SUPERIOR SAMPLE WEIGHT

G.1 DERIVATION OF $\Delta Q(s, u_s)$

Given the greedy action $\hat{\mathbf{u}}$ and a superior action \mathbf{u}_s (i.e. $Q(s, \mathbf{u}_s) > Q(s, \hat{\mathbf{u}})$) assuming $Q(s, \hat{\mathbf{u}}) > 0$ (i.e. $Q_{its}(s, \mathbf{u}) = (1 - \alpha)Q(\hat{\mathbf{u}}, \boldsymbol{\tau})$ for inferior samples), under the hardest exploration case where $\hat{u}^a \neq u_s^a (\forall a \in [1, n])$, the utility function of individual action $u_s^a (a \in [1, n])$ is consist of two parts

$$\begin{aligned} \mathcal{U}^a(u_s^a, \tau^a) = & (1 - \eta_{1,w}) \left[(1 - \alpha)Q(\hat{\mathbf{u}}, \boldsymbol{\tau}) - \sum_k^{m^{n-1}-1} \left[\frac{p(u_s^a, u_k^{-a})}{p(u_s^a) - p(\mathbf{u}_s)} \sum_i^{-a} \mathcal{U}^i(u_k^i, \tau^i) \right] \right] \\ & + \eta_{1,w} \left[Q_{its}(s, \mathbf{u}_s) - \sum_i^{-a} \mathcal{U}^i(u_s^i, \tau^i) \right] \end{aligned} \quad (45)$$

where $\eta_{1,w} = \frac{w\eta_1}{1+(w-1)\eta_1}$, $\eta_1 = (\frac{\epsilon}{m})^{n-1}$ and w is a sample weight on the superior samples. Please refer to Eq.25 for more details about the notations. According to Eq.26, we have

$$\begin{aligned} & \sum_k^{m^{n-1}-1} \left[\frac{p(u_s^a, u_k^{-a})}{p(u_s^a) - p(\mathbf{u}_s)} \sum_i^{-a} \mathcal{U}^i(u_k^i, \tau^i) \right] \\ & = \frac{1}{(1 - \eta_1)} \sum_k^{m^{n-1}-1} \left[\frac{p(u_s^a, u_k^{-a})}{p(u_s^a)} \sum_i^{-a} \mathcal{U}^i(u_k^i, \tau^i) \right] - \frac{\eta_1}{(1 - \eta_1)} \sum_i^{-a} \mathcal{U}^i(u_s^i, \tau^i) \end{aligned} \quad (46)$$

Substituting the left side of Eq.46 into Eq.25

$$\begin{aligned} \mathcal{U}^a(u_s^a, \tau^a) = & (1 - \eta_{1,w})(1 - \alpha)Q(\hat{\mathbf{u}}, \boldsymbol{\tau}) - \frac{1 - \eta_{1,w}}{1 - \eta_1} \sum_k^{m^{n-1}-1} \left[\frac{p(u_s^a, u_k^{-a})}{p(u_s^a)} \sum_i^{-a} \mathcal{U}^i(u_k^i, \tau^i) \right] \\ & + \frac{\eta_1 - \eta_{1,w}}{1 - \eta_1} \sum_i^{-a} \mathcal{U}^i(u_s^i, \tau^i) + \eta_{1,w} Q_{its}(s, \mathbf{u}_s) \end{aligned} \quad (47)$$

Notice that

$$\sum_{a=1}^n \sum_i^{-a} \mathcal{U}^i(u_s^i, \tau^i) = (n - 1) \sum_{a=1}^n \mathcal{U}^i(u_s^i, \tau^i) = (n - 1)Q(\mathbf{u}_s, \boldsymbol{\tau}) \quad (48)$$

The joint Q value function $Q(\mathbf{u}_s, \boldsymbol{\tau})$ can be acquired

$$\begin{aligned} Q(\mathbf{u}_s, \boldsymbol{\tau}) = & \sum_{a=1}^n \mathcal{U}^a(u_s^a, \tau^a) = n(1 - \eta_{1,w})(1 - \alpha)Q(\hat{\mathbf{u}}, \boldsymbol{\tau}) + (n - 1) \frac{\eta_1 - \eta_{1,w}}{1 - \eta_1} Q(\mathbf{u}_s, \boldsymbol{\tau}) \\ & + n\eta_{1,w} Q_{its}(s, \mathbf{u}_s) - \frac{1 - \eta_{1,w}}{1 - \eta_1} \sum_{a=1}^n \sum_k^{m^{n-1}-1} \left[\frac{p(u_s^a, u_k^{-a})}{p(u_s^a)} \sum_i^{-a} \mathcal{U}^i(u_k^i, \tau^i) \right] \end{aligned} \quad (49)$$

According to Eq.30, we have

$$\sum_{a=1}^n \sum_k^{m^{n-1}-1} \left[\frac{p(\hat{u}^a, u_k^{-a})}{p(\hat{u}^a)} \sum_i^{-a} \mathcal{U}^i(u_k^i, \tau^i) \right] = n(1 - \eta_2)(1 - \alpha)Q(\hat{\mathbf{u}}, \boldsymbol{\tau}) + n\eta_2 Q(s, \hat{\mathbf{u}}) - Q(\hat{\mathbf{u}}, \boldsymbol{\tau}) \quad (50)$$

Substituting the left side of Eq.50 into Eq.49

$$\left[1 - (n-1)\frac{\eta_1 - \eta_{1,w}}{1 - \eta_1}\right] Q(\mathbf{u}_s, \boldsymbol{\tau}) = n(1 - \eta_{1,w})(1 - \alpha)Q(\hat{\mathbf{u}}, \boldsymbol{\tau}) + n\eta_{1,w}\mathcal{Q}_{its}(s, \mathbf{u}_s) - \frac{1 - \eta_{1,w}}{1 - \eta_1} [n(1 - \eta_2)(1 - \alpha) - 1] Q(\hat{\mathbf{u}}, \boldsymbol{\tau}) - n\eta_2 \frac{1 - \eta_{1,w}}{1 - \eta_1} \mathcal{Q}(s, \hat{\mathbf{u}}) \quad (51)$$

where $\eta_2 = (1 - \epsilon + \frac{\epsilon}{m})^{n-1}$. Eq.52 can be further simplified as

$$Q(\mathbf{u}_s, \boldsymbol{\tau}) = \frac{n(1 - \alpha)(\eta_2 - \eta_1) + 1}{1 + n(w-1)\eta_1} Q(\hat{\mathbf{u}}, \boldsymbol{\tau}) + n \frac{w(1 + e_Q)\eta_1 - \eta_2}{1 + n(w-1)\eta_1} \mathcal{Q}(s, \hat{\mathbf{u}}) \quad (52)$$

Therefore,

$$\Delta Q(\mathbf{u}_s, \boldsymbol{\tau}) = Q(\mathbf{u}_s, \boldsymbol{\tau}) - Q(\hat{\mathbf{u}}, \boldsymbol{\tau}) = n \frac{(1 - \alpha)(\eta_2 - \eta_1) - (w-1)\eta_1}{1 + n(w-1)\eta_1} Q(\hat{\mathbf{u}}, \boldsymbol{\tau}) + n \frac{w(1 + e_Q)\eta_1 - \eta_2}{1 + n(w-1)\eta_1} \mathcal{Q}(s, \hat{\mathbf{u}}) \quad (53)$$

When $w = 1$, Eq.53 degenerate to Eq.31 (i.e., the case without sample weight). For monotonic value decomposition, Eq.53 also holds since the expressions of $Q(\hat{\mathbf{u}}, \boldsymbol{\tau})$ and $Q(\mathbf{u}_s, \boldsymbol{\tau})$ do not change.

When $\Delta Q(\mathbf{u}_s, \boldsymbol{\tau}) > 0$, $\arg\max_{\mathbf{u}} Q(\mathbf{u}, \boldsymbol{\tau}) \neq \hat{\mathbf{u}}$, which suggests current greedy action is unstable. If $\hat{\mathbf{u}}$ is a non-optimal action, to destabilize it, let $\Delta Q(\mathbf{u}_s, \boldsymbol{\tau}) > 0$, assuming $Q(\hat{\mathbf{u}}, \boldsymbol{\tau}) \approx \mathcal{Q}(s, \hat{\mathbf{u}})$ we have

$$w > \frac{\alpha(\eta_2 - \eta_1)}{e_Q \eta_1} \quad (54)$$

When $\mathbf{u}_s = \arg\max_{\mathbf{u}} \mathcal{Q}(s, \mathbf{u})$, we obtain the lower bound of w , which suggest the non-optimal stable points can be eliminated by a large enough weight on the superior sample under ITS.

G.2 VERIFICATION OF THE EFFECT OF SUPERIOR SAMPLE WEIGHTS UNDER ITS.

We carry out experiments in matrix games to evaluate the effect of the weight on the superior sample under ITS, where the payoff matrix is defined as

$$\mathcal{Q}_{its} = \begin{cases} 6(1 + e_Q) & \mathbf{u} = \{0, 0\} \\ 6 & \mathbf{u} = \{2, 2\} \\ \text{random}(-20, 6) & \text{others} \end{cases} \quad (55)$$

An introduction of the matrix game can be found in the experimental part. An mlp shared by all agents is adopted as the agent network, which is trained for 1000 iterations (100 episodes per iteration) over 5 seeds, where $\alpha = 0.1$, $\epsilon = 0.2$ and $e_Q = 1/3$.

m^n	3^2	5^2	10^2	3^3	3^4
Calculated w_0 (Eq.54)	3.60	6.00	12.00	50.32	659.50
Tested $\Delta Q(\mathbf{u}_s, \boldsymbol{\tau})$ (Eq.53)	0.01 \pm 0.06	0.02 \pm 0.16	0.22 \pm 0.13	-0.02 \pm 0.30	-0.48 \pm 0.75
Tested $Q(\hat{\mathbf{u}}, \boldsymbol{\tau})$	5.95 \pm 0.02	5.97 \pm 0.02	5.98 \pm 0.01	5.90 \pm 0.06	5.93 \pm 0.03

Table 3: Evaluation of the sample weight on superior samples for LVD under ITS. w_0 denotes the lower bound of required sample weight to eliminate the non-optimal stable points when $\Delta Q(\mathbf{u}_s, \boldsymbol{\tau}) = 0$. m is the individual action space size and n is the number of agents.

From Table3, the joint Q value of greedy action approximately equals to its true Q value (i.e., $Q(\hat{\mathbf{u}}, \boldsymbol{\tau}) \approx \mathcal{Q}(s, \hat{\mathbf{u}}) = 6$) under ITS. Besides, the required sample weight to eliminate the non-optimal stable points grows **exponentially** as the number of agent grows, which introduces instability in the joint Q values.

H LVD AND MVD UNDER ITS WITH SUPERIOR EXPERIENCE REPLAY

Given the greedy action $\hat{\mathbf{u}}$ and a superior action \mathbf{u}_s (i.e. $Q(s, \mathbf{u}_s) > Q(s, \hat{\mathbf{u}})$) assuming $Q(s, \hat{\mathbf{u}}) > 0$ (i.e. $Q_{its}(s, \mathbf{u}) = (1 - \alpha)Q(\hat{\mathbf{u}}, \boldsymbol{\tau})$ for inferior samples), under the hardest exploration case where $u_s^a \neq \hat{u}^a (\forall a \in [1, n])$, the utility function of individual action $u_s^a (a \in [1, n])$ is consist of two parts

$$\begin{aligned} \mathcal{U}^a(u_s^a, \tau^a) = & (1 - \eta_{1,ser}) \left[(1 - \alpha)Q(\hat{\mathbf{u}}, \boldsymbol{\tau}) - \sum_k^{m^{n-1}-1} \left[\frac{p(u_s^a, u_k^{-a})}{p(u_s^a) - p(\mathbf{u}_s)} \sum_i^{-a} \mathcal{U}^i(u_k^i, \tau^i) \right] \right] \\ & + \eta_{1,ser} \left[Q_{its}(s, \mathbf{u}_s) - \sum_i^{-a} \mathcal{U}^i(u_s^i, \tau^i) \right] \end{aligned} \quad (56)$$

where $\eta_{1,ser} = \frac{w+\eta_1}{1+w}$, $\eta_1 = (\frac{\epsilon}{m})^{n-1}$ and w is a sample weight on the superior samples from the superior buffer. Please refer to Eq.25 for more details about the notations. Following the derivation provided in Appendix G.1, we have

$$\begin{aligned} \left[1 - (n-1) \frac{\eta_1 - \eta_{1,ser}}{1 - \eta_1} \right] Q(\mathbf{u}_s, \boldsymbol{\tau}) = & n(1 - \eta_{1,ser})(1 - \alpha)Q(\hat{\mathbf{u}}, \boldsymbol{\tau}) + n\eta_{1,ser}Q_{its}(s, \mathbf{u}_s) \\ & - \frac{1 - \eta_{1,ser}}{1 - \eta_1} [n(1 - \eta_2)(1 - \alpha) - 1] Q(\hat{\mathbf{u}}, \boldsymbol{\tau}) - n\eta_2 \frac{1 - \eta_{1,ser}}{1 - \eta_1} Q(s, \hat{\mathbf{u}}) \end{aligned} \quad (57)$$

Eq.57 can be further simplified as

$$Q(\mathbf{u}_s, \boldsymbol{\tau}) = \frac{n(1 - \alpha)(\eta_2 - \eta_1) + 1}{1 + nw} Q(\hat{\mathbf{u}}, \boldsymbol{\tau}) + n \frac{(w + \eta_1)(1 + e_Q) - \eta_2}{1 + nw} Q(s, \hat{\mathbf{u}}) \quad (58)$$

where $\eta_2 = (1 - \epsilon + \frac{\epsilon}{m})^{n-1}$. Therefore,

$$\begin{aligned} \Delta Q(\mathbf{u}_s, \boldsymbol{\tau}) = Q(\mathbf{u}_s, \boldsymbol{\tau}) - Q(\hat{\mathbf{u}}, \boldsymbol{\tau}) = & n \frac{(1 - \alpha)(\eta_2 - \eta_1) - w}{1 + nw} Q(\hat{\mathbf{u}}, \boldsymbol{\tau}) \\ & + n \frac{(w + \eta_1)(1 + e_Q) - \eta_2}{1 + nw} Q(s, \hat{\mathbf{u}}) \end{aligned} \quad (59)$$

When $w = 0$, Eq.59 degenerate to Eq.31 (i.e., the case without samples form superior buffer). For monotonic value decomposition, Eq.59 also holds since the expressions of $Q(\hat{\mathbf{u}}, \boldsymbol{\tau})$ and $Q(\mathbf{u}_s, \boldsymbol{\tau})$ do not change.

If $\hat{\mathbf{u}}$ is a non-optimal action, to destabilize it, let $\Delta Q(\mathbf{u}_s, \boldsymbol{\tau}) > 0$. A sufficient condition for $\Delta Q(\mathbf{u}_s, \boldsymbol{\tau}) > 0$ is both terms in the right side of Eq.59 are no less than 0. As a result,

$$\frac{\eta_2}{1 + e_Q} - \eta_1 \leq w \leq (1 - \alpha)(\eta_2 - \eta_1) \quad (60)$$

To ensure $\frac{\eta_2}{1 + e_Q} - \eta_1 < \frac{\eta_2}{1 + e_Q} - \eta_1$, let $\alpha = \frac{e_Q}{1 - e_Q}$. According to Eq.60, **SER can eliminate the non-optimal stable points by a selecting a suitable value of w for superior samples.**

I WORKING PRINCIPLE OF GVR AND THE ALGORITHM

Examples of ITS target is provided in Fig.8. The working principle of GVR is shown in Fig.9. The algorithm is given in Algo.1. For details about notations please refer to Appendix H.

8	-12	-12
-12	0	0
-12	0	6
$Q(s, \mathbf{u})$		

	\mathbf{u}	$\{0, 0\}$	$\{1, 1\}$	$\{2, 2\}$
$\mathcal{V}_{gvr}(s) = Q(s, \mathbf{u}) * (1 + e_{Q0})$		8.8	0	6.6
$Q(\mathbf{u}, \tau)$		7.8	-0.2	5.8
$Q_{its}(s, \mathbf{u})$ for inferior actions ($Q(\mathbf{u}, \tau) - \alpha Q(\mathbf{u}, \tau) $)		6.93	-0.22	5.16

8	6.93	6.93
6.93	6.93	6.93
6.93	6.93	6.93

$Q_{its}(s, \mathbf{u})$
under $\mathbf{u} = \{0, 0\}$

8	-0.22	-0.22
-0.22	0	0
-0.22	0	6

$Q_{its}(s, \mathbf{u})$
under $\mathbf{u} = \{1, 1\}$

8	5.16	5.16
5.16	5.16	5.16
5.16	5.16	6

$Q_{its}(s, \mathbf{u})$
under $\mathbf{u} = \{2, 2\}$

■ greedy action
■ inferior action
■ superior action

Figure 8: Examples of ITS target, where $e_{Q0} = 0.1$ and $\alpha = 0.11$.

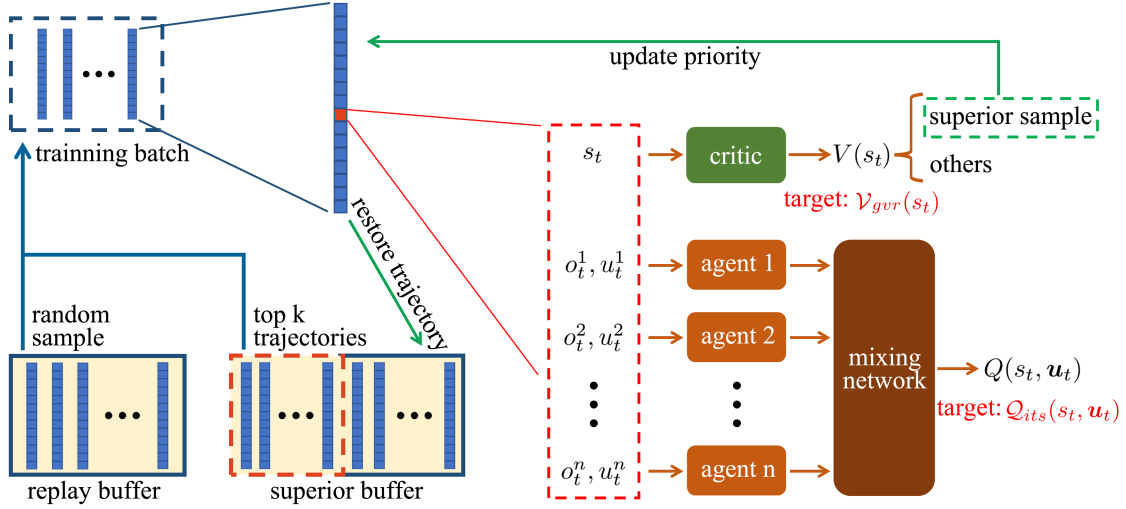


Figure 9: The working principle of GVR. In the training stage of each iteration, we acquire the training batch by concatenating the trajectories sampled from the replay buffer and the superior buffer. Then we calculate the loss of $Q(\mathbf{u}, \tau)$ and $V(s)$ referring to their targets. After that, we update the priority of the trajectories in training batch and restore the trajectories to the superior buffer according to the updated priority.

J EFFECT OF REWARD FUNCTION AND ϵ ON STABLE POINTS.

We conduct experiments in two-agent matrix games to verify the effect of reward function and ϵ on stable points. An mlp shared by two agents is adopted as the agent network. The ratios of different stable points are counted with ϵ increasing from 0 to 0.99. At each value of ϵ , 100 times of independent training and test are executed. Each training includes 2000 episodes. The experiments are carried out over 5 seeds. According to Fig.10, the stable points changes with both true Q value and ϵ . As ϵ grows, there becomes only one stable point. We ignore situations with non-unique optimal stable points (e.g., $[[1,0],[0,1]]$), where the stable points can also be calculated referring to Eq.19.

Algorithm 1 Greedy-based Value Representation

Initialize parameters θ_a for agents and θ_c for critic
 Initialize replay buffer D_r and superior buffer D_s
 Initialize hyper-parameter e_{Q0} , $\alpha = \frac{e_{Q0}}{1-e_{Q0}}$, weight $w = (1 - \alpha)(\eta_2 - \eta_1)$
for iteration $i = 1, 2, 3, \dots$ **do**
 Interact with environment and store transitions to D_r
 Sample batch b_r from D_r
 Take out the top-k trajectories b_s from D_s
 Concat batches $b_{total} = b_r + b_s$
 for trajectory $\tau = 1, 2, 3, \dots$ in b_{total} **do**
 Calculate critic loss $loss_c = |\mathcal{Q}(s, \mathbf{u}) - V_{\theta_c}(s)|_2 * \mathcal{I}(\mathbf{u} = \hat{\mathbf{u}})$
 if trajectory is from b_s **then**
 Calculate agent loss for superior samples $loss_a = w|\mathcal{Q}_{its}(s, \mathbf{u}) - Q_{\theta_a}(\mathbf{u}, \tau)|_2 * \mathcal{I}(\mathcal{Q}(s, \mathbf{u}) > V_{\theta_c}(s))$
 else
 Calculate agent loss $loss_a = |\mathcal{Q}_{its}(s, \mathbf{u}) - Q_{\theta_a}(\mathbf{u}, \tau)|_2$
 end if
 Update priority p_τ
 Restore τ to D_b according to p_τ
 end for
 Update θ_a and θ_c
end for

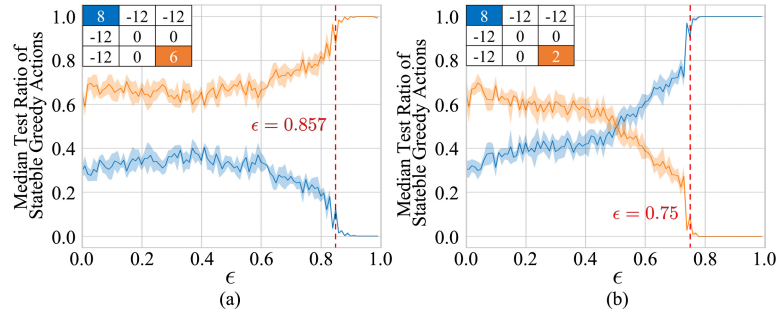


Figure 10: Median test ratios of stable points (i.e., test probability of different convergence) under 100 times of independent training vs ϵ . The payoff matrices are shown in the upper-left of each subgraph. The greedy actions in different stable points are marked with different colors (blue for $\{u^1, u^2\} = \{0, 0\}$ and orange for $\{u^1, u^2\} = \{2, 2\}$). Take subgraph (a) as an example, when $\epsilon = 0.4$, the ratios of two stable greedy actions ($\{0, 0\}$ and $\{2, 2\}$) approximate 0.35 and 0.65 respectively. In the presented examples, when $\epsilon > 0.857$ and $\epsilon > 0.75$, there becomes **almost only one stable point, which consists with the calculated threshold** (denoted by red dash lines) from Eq.19.

K EXPERIMENTAL SETTINGS AND ADDITIONAL EXPERIMENTS

K.1 ABLATION STUDIES

We conduct ablation studies to investigate the effect of GVR. We first evaluate the effect of inferior target shaping (ITS) and superior experience replay (SER) on QMIX. The experimental settings are the same as the comparative experiments of predator-prey before. The experiments are carried out over 5 seeds.

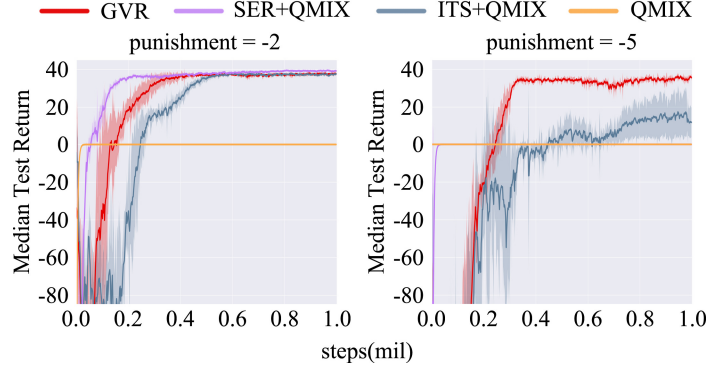


Figure 11: Ablation studies on the effect of ITS and SER.

It can be seen from the Fig.11 that in task with punishment -2, both ITS and SER helps to solve the problem. In task with punishment -5, due to the extreme negative return of inferior samples, SER alone is unable to solve the problem. Meanwhile, in spite of the shaped reward by ITS, the proportion of superior samples is very small, leading to instability during training.

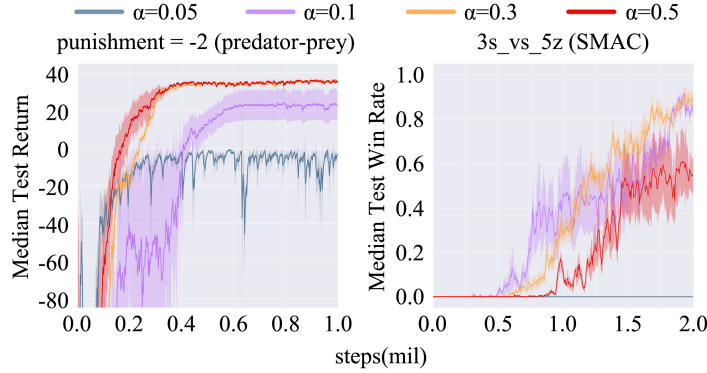


Figure 12: Ablation studies on the parameter α .

We also investigate the effect of the parameter α on GVR. The experimental settings for SMAC and predator-prey are the same as the corresponding comparative experiments before. The experiments are carried out over 5 seeds.

It can be seen from the Fig.12 that a too small or too large value of α leads to poor performance. According to the definition of ITS target, the α determines the gap the joint Q values between greedy samples and inferior samples. As a result, a too-small value of α brings the risk of confusion between these two kinds of samples. Meanwhile, a too-big value of α may prevent the update from a greedy action to a superior action.

K.2 COMPARISON WITH JOINT EXPLORATION METHODS

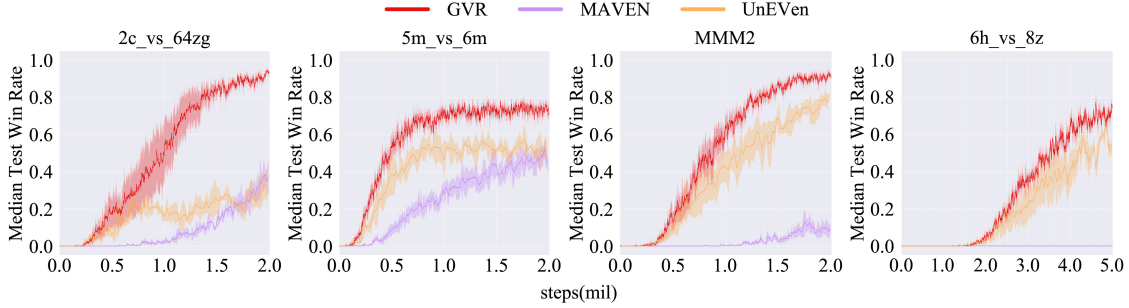


Figure 13: Comparison between GVR, MAVEN and UneVen.

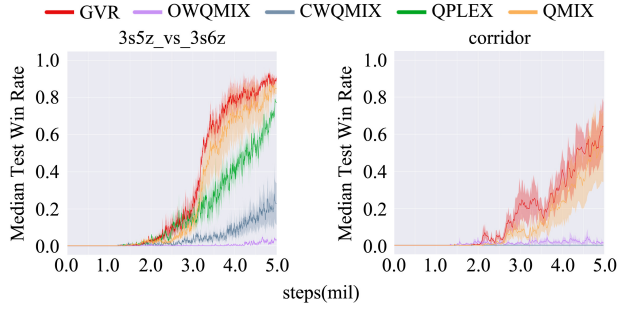


Figure 14: Comparison between GVR and baselines on two super hard SMAC tasks.

We compare our method with MAVEN and UneVen on SMAC. The experiment results are given in Fig.13, where GVR shows the best performance. Besides, to further investigate the scalability of our method, we investigate the performance of GVR on two other super hard tasks of SMAC, and the experiment results are shown in Fig.14.

L LIMITATIONS

L.1 THE WORST CASE

In GVR, we consider the situations with unique superior action, where the worst cases are ignored. For situations with multiple superior actions $\{\mathbf{u}_{s,1}, \dots, \mathbf{u}_{s,p}\}$, two examples where Eq.32 fails to eliminate the non-optimal stable points are given in Fig.15, where the superior actions ($\{\mathbf{u}_{s,1}, \dots, \mathbf{u}_{s,p}\}$) and greedy action ($\hat{\mathbf{u}}$) are denoted by block of blue and red respectively.

In both examples, $u_{s,i}^k \neq u_{s,j}^k, \forall k \in [1, n], \forall i, j \in [1, p]$ and $i \neq j$, which suggest $\mathbf{u}_{s,i}$ do not affect $Q(\mathbf{u}_{s,j}, \boldsymbol{\tau})$. However, according to Eq.39, $Q(\hat{\mathbf{u}}, \boldsymbol{\tau})$ is increased since each superior action shares individual actions with the greedy action.

A method to avoid these situations in GVR is setting the batch size of superior batch (i.e., the batch sampled from the superior buffer) to 1, which may reduce the effect of GVR. In practice, we ignore these cases since the probability of such cases are very small.

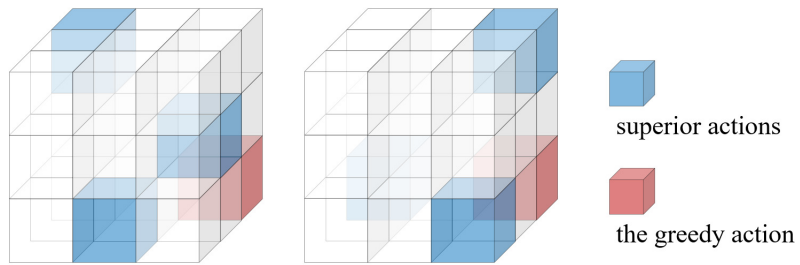


Figure 15: Examples of multiple superior actions in 3-agent cooperation.

L.2 DISCUSSION: TRADE-OFF BETWEEN OPTIMALITY AND STABILITY